European Journal of Mechanics A/Solids 28 (2009) 387–401

Contents lists available at ScienceDirect

European Journal of Mechanics A/Solids

www.elsevier.com/locate/ejmsol

A finite-strain model for anisotropic viscoplastic porous media: I – Theory

K. Danas[a,b], P. Ponte Castañeda[a,b,*]

[a] Department of Mechanical Engineering and Applied Mechanics, University of Pennsylvania, Philadelphia, PA 19104-6315, USA
[b] Laboratoire de Mécanique des Solides, C.N.R.S. UMR 7649, Département de Mécanique, École Polytechnique, 91128 Palaiseau Cedex, France

A R T I C L E I N F O

Article history:
Received 17 July 2008
Accepted 7 November 2008
Available online 12 November 2008

Keywords:
Porous media
Homogenization
Viscoplastic
Constitutive model
Microstructure evolution

A B S T R A C T

In this work, we propose an approximate homogenization-based constitutive model for estimating the effective response and associated microstructure evolution in viscoplastic (including ideally-plastic) porous media subjected to finite-strain loading conditions. The proposed model is based on the "second-order" nonlinear homogenization method, and is constructed in such a way as to reproduce exactly the behavior of a "composite-sphere assemblage" in the limit of hydrostatic loading and isotropic microstructure. However, the model is designed to hold for completely general three-dimensional loading conditions, leading to deformation-induced anisotropy, whose development in time is handled through evolution laws for the internal variables characterizing the instantaneous "ellipsoidal" state of the microstructure. In Part II of this study, results will be given for the instantaneous response and microstructure evolution in porous media for several representative loading conditions and microstructural configurations.

1. Introduction

This work is intended to provide an approximate homogenization-based model for the prediction of the effective behavior and microstructure evolution of anisotropic viscoplastic (and ideally-plastic) porous materials subjected to general three-dimensional loading conditions. Even though, in several cases, these materials can be regarded as initially isotropic, it is well understood by now that when they are subjected to finite deformations, their microstructure evolves leading to an overall anisotropic response. From this viewpoint, the main purpose of this study is to develop constitutive models for viscoplastic porous materials that are capable of handling the nonlinear response of the porous medium, microstructural information, such as the volume fraction, the average shape and orientation of the voids, the evolution of the underlying microstructure and possible development of instabilities. Moreover, these models need to be simple and robust enough to be easily implemented in finite element codes.

In this quest, numerous constitutive theories and models have been proposed in the last forty years. Possibly, these studies could be classified in two main groups; those concerned with a dilute concentration of voids and those dealing with finite porosities. In the first group of dilute porous media, major contributions are due to McClintock (1968), Rice and Tracey (1969), Budiansky et al. (1982), Duva and Hutchinson (1984), Fleck and Hutchinson (1986), Duva (1986) and Lee and Mear (1992a, 1992b, 1994, 1999). These methods are based on the minimum principle of velocities as stated by Hill (1956), as well as on the choice of a stream function via the Rayleigh–Ritz procedure allowing for the description of the actual field in terms of an approximate field consisting of a sum of linearly independent functions. A significant application of these techniques is associated with cavitation instabilities in metal-matrix materials (Huang, 1991; Huang et al., 1991), where a sudden increase of initially small voids can cause failure of the medium at high stress triaxial loads. Nevertheless, the extension of these methodologies to general three-dimensional ellipsoidal microstructures and loading conditions is not straightforward, due to the fact that the stream function technique is restricted to problems with two-dimensional character, such as for porous media with cylindrical voids of circular or elliptical cross-sections, as well as for porous materials consisting of spheroidal voids subjected to axisymmetric loading conditions (aligned with the pore symmetry axis). Nonetheless, these limitations do not eliminate the usefulness of such methods, which were able to predict interesting nonlinear effects to be discussed in Part II of this work.

In the second group of porous media with finite porosities, we distinguish first the well-known work of Gurson (1977), who makes use of the exact solution for a shell (spherical or cylindrical cavity) under hydrostatic loadings, suitably modified, to obtain estimates for the effective behavior of ideally-plastic solids with isotropic or transversely isotropic distributions of porosity. In this context, Aravas (1987) has successfully developed a numerical integration scheme for elasto-plastic porous media based on the Gurson model, which is widely used in commercial applications. On

* Corresponding author. Tel.: +1 215 898 5046; fax: +1 215 573 6334.
E-mail addresses: kdanas@seas.upenn.edu (K. Danas), ponte@seas.upenn.edu (P. Ponte Castañeda).

0997-7538/$ – see front matter
doi:10.1016/j.euromechsol.2008.11.002

the other hand, Tvergaard (1981) found that the Gurson model is stiff when compared with finite element unit-cell calculations. To amend this, the same author proposed a modification of the Gurson criterion, by introducing an ad-hoc scalar factor, which led to more compliant estimates. In turn, the Gurson model was generalized to isotropic viscoplastic porous materials by Leblond et al. (1994).

Even though the Gurson model has been shown to deliver sufficiently accurate predictions for isotropic porous solids under high triaxial loads, it contains no information about the shape of the voids and thus is expected to give very poor estimates in the case of low and moderate triaxial loadings. In an attempt to overcome this otherwise important shortcoming of the model, Gologanu et al. (1993, 1994, 1997) and later Gărăjeu et al. (2000), Flandi and Leblond (2005a, 2005b) and Monchiet et al. (2007) proposed improved Gurson-type criteria for porous media with an ideally-plastic and viscoplastic matrix phase, which made use of a *spheroidal shell* containing a confocal spheroidal void (leading to transversely isotropic symmetry for the material) subjected to *axisymmetric* loading conditions aligned with the pore symmetry axis. These refined criteria allowed these authors to study successfully practical problems of interest involving coalescence of voids at high triaxial loadings. Nonetheless, all these studies are based on prescriptions for a trial velocity field similar to the dilute stream function methods discussed earlier. For this reason, an extension of these techniques to more general microstructures and loading conditions is not simple and—to the best knowledge of the authors—there exist no results for such more general cases.

Based on *nonlinear homogenization techniques*, an alternative class of constitutive models for dilute and non-dilute porous materials that are capable of handling general "ellipsoidal" microstructures (i.e., particulate microstructures with more general orthotropic overall anisotropy) and general three-dimensional loading conditions (including nonaligned loadings) has been developed in the last twenty years. More specifically, following the work of Willis (1977, 1978) on linear composites, Talbot and Willis (1985) used a "linear homogeneous comparison" material to provide a generalization of the Hashin–Shtrikman bounds (Hashin and Shtrikman, 1963) in the context of nonlinear composites. A more general class of nonlinear homogenization methods has been introduced by Ponte Castañeda (1991, 1992) (see also Willis (1991)), who obtained rigorous bounds by making use—via a suitably designed variational principle—of an optimally chosen "linear comparison composite" (LCC) with the same microstructure as the nonlinear composite. Michel and Suquet (1992) and Suquet (1993) derived independently an equivalent bound for two-phase power-law media using Hölder-type inequalities, while Suquet (1995) made the observation that the optimal linearization in the "variational" bound (*VAR*) of Ponte Castañeda (1991) is given by the *secant moduli* evaluated at the second moments of the local fields in each phase in the LCC.

Because the *VAR* method delivers a rigorous bound, it tends to be relatively stiff for the effective behavior of nonlinear composites. In this connection, Ponte Castañeda (2002a) proposed the "second-order" method (*SOM*), which made use of more general types of linear comparison composites (anisotropic thermoelastic phases). While the *VAR* method provides a rigorous bound, the *SOM* method delivers stationary estimates. In addition, the optimal linearization in the *SOM* method, which improves significantly on the previous methods, is identified with *generalized-secant moduli* of the phases that depend on both the first and the second moments of the local fields. The main conclusions drawn by these and other works (Ponte Castañeda and Zaidman, 1994; Ponte Castañeda and Suquet, 1998; Ponte Castañeda, 2002b) is that the LCC-based methods lead to estimates that are, in general, more accurate than those resulting from the earlier methodologies mentioned above. However, all of these LCC estimates remain overly stiff in the case of porous viscoplastic materials, particularly for high triaxial loadings (Ponte Castañeda and Zaidman, 1994; Pastor and Ponte Castañeda, 2002). As suggested in Ponte Castañeda and Suquet (1998) and demonstrated in Bilger et al. (2002) for a composite-sphere assemblage, the "variational" estimates may be improved by discretizing the modulus of the matrix phase in the LCC. However, this approach is much more difficult to implement for more general microstructures.

In this context, the main objective of this work is to propose a general, three-dimensional model based on the *SOM* nonlinear homogenization method of Ponte Castañeda (2002a) to estimate *accurately* the effective behavior of anisotropic viscoplastic porous solids subjected to finite deformations. One of the main issues in this study is the improvement of this new model relative to the earlier *VAR* method for high triaxiality loading conditions, while still being able to *handle completely general loading conditions and ellipsoidal microstructures*. Then, building on prior work by Ponte Castañeda and Zaidman (1994), Kailasam and Ponte Castañeda (1998) and Aravas and Ponte Castañeda (2004), the model is also complemented with appropriate evolution laws for the internal variables characterizing the underlying microstructure.

In Part I of this work, we present the theoretical issues associated with the proposed constitutive model, while in Part II we attempt to validate the model against finite element unit-cell calculations, as well as to present representative results that evidence the importance of being able to handle general ellipsoidal microstructures and loading conditions. Specifically, in Section 2 of this paper, we pose the problem under consideration by identifying two distinct procedures; (a) the prediction of the *instantaneous* effective behavior of the porous material and (b) the evolution of microstructure during the deformation process. In Section 3, we describe the homogenization model by making use of the *SOM* and by extending the work of Danas et al. (2008a, 2008b) for isotropic and transversely isotropic porous media to general ellipsoidal microstructures. Section 4 presents the evolution laws for the internal variables that are used to describe the underlying microstructure. Section 5 is devoted to the special case of porous media with an ideally-plastic matrix phase. Finally, Appendix D presents the numerical integration of the equations describing the instantaneous effective behavior and microstructure evolution of the porous material subjected to finite deformations.

2. Problem setting

Consider a representative volume element (RVE) Ω of a two-phase porous medium with each phase occupying a sub-domain $\Omega^{(r)}$ $(r = 1, 2)$. It is important to note that the RVE is much larger than the size of the typical heterogeneity in the solid, i.e., it satisfies the "separation of the length scale" hypothesis (Hill, 1963).

Local constitutive behavior. Let the vacuous phase be identified with phase 2 and the nonvacuous phase (i.e., matrix phase) with phase 1. For later reference, the brackets $\langle\cdot\rangle$ and $\langle\cdot\rangle^{(r)}$ are used to denote volume averages over the RVE (Ω) and the phase r ($\Omega^{(r)}$), respectively. While the stress potential of the porous phase $U^{(2)}$ is equal to zero, the local behavior of the matrix phase is characterized by a convex, incompressible, isotropic stress potential $U \equiv U^{(1)}$, such that the Cauchy stress $\boldsymbol{\sigma}$ and the Eulerian strain-rate $\boldsymbol{D}$ at any point in $\Omega^{(1)}$ are related by

$$\boldsymbol{D} = \frac{\partial U}{\partial \boldsymbol{\sigma}}(\boldsymbol{\sigma}), \quad \text{with } U(\boldsymbol{\sigma}) = \frac{\dot{\varepsilon}_o \sigma_o}{n+1}\left(\frac{\sigma_{\text{eq}}}{\sigma_o}\right)^{n+1}, \quad n = \frac{1}{m}. \tag{1}$$

The von Mises equivalent stress is defined in terms of the deviatoric stress tensor $\boldsymbol{\sigma}'$ as $\sigma_{\text{eq}} = \sqrt{\frac{3}{2}\boldsymbol{\sigma}' \cdot \boldsymbol{\sigma}'}$, and σ_o and $\dot{\varepsilon}_o$ denote the flow stress and reference strain-rate of the matrix phase,

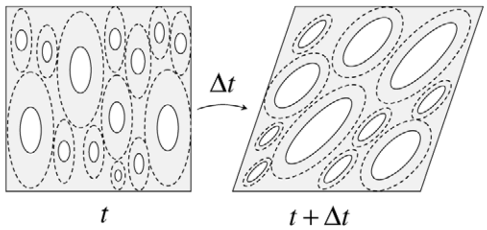

Fig. 1. Representative volume element of a "particulate" porous medium at two given instants. The ellipsoidal voids are distributed randomly with "ellipsoidal symmetry." The solid ellipsoids denote the voids, and the dashed ellipsoids, their distribution.

respectively. The nonlinearity of the matrix phase is introduced through m, which denotes the strain-rate sensitivity parameter and takes values between 0 and 1. Note that the two limiting values $m=1$ (or $n=1$) and $m=0$ (or $n\to\infty$) correspond to linear and ideally-plastic behaviors, respectively.

2.1. Description of the microstructure

Due to the Eulerian kinematics used for the description of the phases, it is appropriate to adopt an incremental formalism for the solution of the finite deformation problem. At a given instant in time t, we take a *snapshot* of the microstructure (see Fig. 1) and we attempt to provide an estimate for the *instantaneous* behavior of the material. In the sequel, we update the microstructure and proceed to the next time step $t+\Delta t$. This procedure is repeated until we reach the final prescribed total time. Thus, for the prediction of the instantaneous effective behavior of the porous material, it is necessary to describe, first, the microstructure—at a fixed time t—in terms of certain internal variables.

In this connection, following the work of Willis (1978), we consider a porous material that comprises a matrix phase in which voids of known shapes and orientation are embedded. This description represents a "particulate" microstructure and is a generalization of the Eshelby (1957) dilute microstructure in the non-dilute regime. More specifically, we consider a "particulate" porous material (see Fig. 1) consisting of ellipsoidal voids aligned at a certain direction, whereas the distribution function, which is also taken to be ellipsoidal in shape, provides information about the distribution of the centers of the inclusions. Note that the shape of the distribution function and the shape of the voids need not be identical (Ponte Castañeda and Willis, 1995).

Nevertheless, the effect of the shape and orientation of the distribution function on the effective behavior of the porous material becomes less important at low and moderate porosities (Kailasam and Ponte Castañeda, 1998) due to the fact that the contribution of the distribution function is only of order two in the volume fractions of the voids. This assumption ceases to be valid for conditions leading to void coalescence. For such cases, the contribution of the distribution function to the overall behavior of the porous medium is expected to be rather significant and it should not be neglected. Nonetheless, this work is mainly concerned with low to moderate concentrations of voids prior to coalescence, and for simplicity, we will make the assumption, which will hold for the rest of the text, that the shape and orientation of the distribution function is identical to the shape and orientation of the voids and hence it evolves in the same fashion when the material is subjected to finite deformations. In view of this hypothesis, the basic internal variables characterizing the instantaneous state of the microstructure are:

1. the volume fraction of the voids or porosity $f=\mathcal{V}_2/\mathcal{V}$, where $\mathcal{V}=\mathcal{V}_1+\mathcal{V}_2$ denotes the total volume, with $\mathcal{V}_1$ and $\mathcal{V}_2$ being the volume occupied by the matrix and the vacuous phase, respectively,

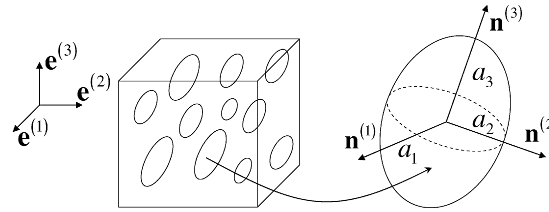

Fig. 2. Representative ellipsoidal void.

2. the two aspect ratios $w_1=a_3/a_1$, $w_2=a_3/a_2$ ($w_3=1$), where $2a_i$ with $i=1,2,3$ denote the lengths of the principal axes of the representative ellipsoidal void,
3. the orientation unit vectors $\mathbf{n}^{(i)}$ ($i=1,2,3$), defining an orthonormal basis set, which coincides with the principal axes of the representative ellipsoidal void.

The above set of the microstructural variables is expediently denoted by

$$s_\alpha=\left\{f,w_1,w_2,\mathbf{n}^{(1)},\mathbf{n}^{(2)},\mathbf{n}^{(3)}=\mathbf{n}^{(1)}\times\mathbf{n}^{(2)}\right\}. \tag{2}$$

A schematic representation of the above-described microstructure is shown in Fig. 2.

Note that as a consequence of the above-defined microstructure the porous medium is, in general, orthotropic, with the axes of orthotropy coinciding with the principal axes of the representative ellipsoidal void, i.e., with $\mathbf{n}^{(i)}$. Nevertheless, some special cases of interest could be identified. Firstly, when $w_1=w_2=1$, the resulting porous medium exhibits an overall isotropic behavior, provided that the matrix phase is also characterized by an isotropic stress potential. Secondly, if $w_1=w_2\neq1$, the corresponding porous medium is transversely isotropic about the $\mathbf{n}^{(3)}$-direction, provided that the matrix phase is isotropic or transversely isotropic about the same direction.

For later reference, it is relevant to explore other types of particulate microstructures, which can be derived easily by appropriate specialization of the aforementioned variables s_α (Budiansky et al., 1982). In this regard, the following cases are considered:

- $a_1\to\infty$ or $a_2\to\infty$ or $a_3\to\infty$. Then, if the porosity f remains finite, the cylindrical microstructure is recovered, whereas if $f\to0$, a porous material with infinitely thin needles is generated.
- $a_1\to0$ or $a_2\to0$ or $a_3\to0$. Then, if the porosity f remains finite, the laminated microstructure is recovered (or alternatively a "porous sandwich"), whereas if $f\to0$, a porous material with penny-shaped cracks is formed and thus the notion of density of cracks needs to be introduced. This special case will not be studied here, rather it will be reported elsewhere.

To summarize, the set of the above-mentioned microstructural variables s_α provides a general three-dimensional description of a particulate porous material. It is evident that in the general case, where the aspect ratios and the orientation of the ellipsoidal voids are such that $w_1\neq w_2\neq1$ and $\mathbf{n}^{(i)}\neq\mathbf{e}^{(i)}$, the porous medium becomes highly anisotropic and estimating the overall response of such materials exactly is a real challenge. However, linear and nonlinear homogenization methods have been developed in the recent years that are capable of providing estimates and bounds for the overall behavior of such particulate composites. In the following subsection, we present a general framework which will allow us to obtain estimates for the instantaneous effective behavior and the microstructure evolution of viscoplastic porous media.

2.2. Instantaneous response and microstructure evolution – preliminaries

Let $\boldsymbol{L}$ $(=\nabla\mathbf{v})$, $\boldsymbol{D}$ and $\boldsymbol{\Omega}$ denote the velocity gradient, strain-rate and spin tensors, respectively. Then, under the affine boundary condition $\mathbf{v}=\bar{\boldsymbol{L}}\mathbf{x}$ on $\partial\Omega$, the corresponding macroscopic quantities are obtained as averages over the representative volume element, $\bar{\boldsymbol{L}}=\langle\boldsymbol{L}\rangle$, $\bar{\boldsymbol{D}}=\langle\boldsymbol{D}\rangle$, and $\bar{\boldsymbol{\Omega}}=\langle\boldsymbol{\Omega}\rangle$, and satisfy the relations

$$\bar{\boldsymbol{D}}=\frac{1}{2}\left(\bar{\boldsymbol{L}}+\bar{\boldsymbol{L}}^T\right) \quad\text{and}\quad \bar{\boldsymbol{\Omega}}=\frac{1}{2}\left(\bar{\boldsymbol{L}}-\bar{\boldsymbol{L}}^T\right). \tag{3}$$

We also define the macroscopic Cauchy stress tensor $\bar{\boldsymbol{\sigma}}=\langle\boldsymbol{\sigma}\rangle$, as well as the stress triaxiality by

$$X_\Sigma=\bar{\sigma}_m/\bar{\sigma}_{eq},\quad \bar{\sigma}_{eq}=\sqrt{3\bar{\boldsymbol{\sigma}}'\cdot\bar{\boldsymbol{\sigma}}'/2},\quad \bar{\sigma}_m=\bar{\sigma}_{ii}/3,\quad i=1,2,3, \tag{4}$$

where $\bar{\sigma}_m$ and $\bar{\sigma}_{eq}$ are the macroscopic hydrostatic and von Mises equivalent stresses, respectively, and $\bar{\boldsymbol{\sigma}}'$ denotes the deviatoric part of the macroscopic stress $\bar{\boldsymbol{\sigma}}$.

The *instantaneous* effective behavior of the porous material is defined as the relation between the average stress, $\bar{\boldsymbol{\sigma}}$, and the average strain-rate, $\bar{\boldsymbol{D}}$, which can also be characterized by an effective stress potential $\tilde{U}$, such that (Hill, 1963)

$$\bar{\boldsymbol{D}}=\frac{\partial\tilde{U}}{\partial\bar{\boldsymbol{\sigma}}}(\bar{\boldsymbol{\sigma}}),\qquad \tilde{U}(\bar{\boldsymbol{\sigma}};s_\alpha)=(1-f)\min_{\boldsymbol{\sigma}\in\mathcal{S}(\bar{\boldsymbol{\sigma}})}\left\langle U(\boldsymbol{\sigma})\right\rangle^{(1)}. \tag{5}$$

In this expression, $\mathcal{S}(\bar{\boldsymbol{\sigma}})=\{\boldsymbol{\sigma},\operatorname{div}\boldsymbol{\sigma}=0 \text{ in } \Omega, \boldsymbol{\sigma}\mathbf{n}=\mathbf{0} \text{ on } \partial\Omega^{(2)}, \langle\boldsymbol{\sigma}\rangle=\bar{\boldsymbol{\sigma}}\}$ denotes the set of statically admissible stresses.

The homogenized constitutive relation (5) provides information about the *instantaneous* effective response of the porous material for a given microstructural configuration s_α. However, these materials are often subjected to finite deformations inducing the evolution of the underlying microstructure. Thus, the instantaneous description (5) needs to be supplemented with evolution laws for the internal variables s_α that characterize the microstructure, i.e.,

$$\dot{s}_\alpha=\mathrm{fcn}(\bar{\boldsymbol{\sigma}},s_\alpha), \tag{6}$$

where the "dot" denotes the standard time derivative.

The above relations provide a general framework for the prediction of the instantaneous effective behavior and microstructure evolution in particulate porous media. Note, however, that the determination of $\tilde{U}$ exactly is an extremely difficult task, in general. In the next section, a homogenization method for estimating $\tilde{U}$ is recalled and applied to the class of particulate viscoplastic porous materials. Before proceeding with the analysis, it is convenient to extract some general information about $\tilde{U}$ by making use of the notion of the "gauge function."

2.3. Gauge function

Using the homogeneity of the local stress potential U in $\boldsymbol{\sigma}$ and of the effective stress potential $\tilde{U}$ in $\bar{\boldsymbol{\sigma}}$ (Suquet, 1993), it is convenient to introduce the so-called gauge factor Γ_n (the subscript being used to denote dependence on the nonlinear exponent n), such that (Leblond et al., 1994)

$$\tilde{U}(\bar{\boldsymbol{\sigma}};s_\alpha)=\frac{\dot{\varepsilon}_o\sigma_o}{n+1}\left(\frac{\Gamma_n(\bar{\boldsymbol{\sigma}};s_\alpha)}{\sigma_o}\right)^{n+1}. \tag{7}$$

It is then sufficient to study only one of the equipotential surfaces $\{\bar{\boldsymbol{\sigma}},\tilde{U}(\bar{\boldsymbol{\sigma}})=const\}$, i.e., the so-called *gauge surface* $\mathcal{P}_n$ of the porous material defined by

$$\mathcal{P}_n\equiv\left\{\bar{\boldsymbol{\Sigma}},\tilde{U}(\bar{\boldsymbol{\Sigma}};s_\alpha)=\frac{\dot{\varepsilon}_o\sigma_o^{-n}}{n+1}\right\}. \tag{8}$$

Consequently, the value of $\tilde{U}$ for any stress tensor $\bar{\boldsymbol{\sigma}}$ is given by (7), with Γ_n satisfying the relation

$$\bar{\boldsymbol{\sigma}}=\Gamma_n(\boldsymbol{\sigma};s_\alpha)\bar{\boldsymbol{\Sigma}}\quad\text{or}\quad \bar{\boldsymbol{\Sigma}}=\frac{\bar{\boldsymbol{\sigma}}}{\Gamma_n(\bar{\boldsymbol{\sigma}};s_\alpha)}. \tag{9}$$

Note that Γ_n is homogeneous of degree one in $\bar{\boldsymbol{\sigma}}$, and therefore $\bar{\boldsymbol{\Sigma}}$ is homogeneous of degree zero in $\bar{\boldsymbol{\sigma}}$.

In view of relation (8) and the definition of the gauge factor Γ_n in (7), it is pertinent to define the *gauge function* $\tilde{\Phi}_n$, which provides the equation for the gauge surface via the expression

$$\bar{\boldsymbol{\Sigma}}\in\mathcal{P}_n\quad\Longleftrightarrow\quad\tilde{\Phi}_n(\bar{\boldsymbol{\Sigma}};s_\alpha)=\Gamma_n(\bar{\boldsymbol{\Sigma}};s_\alpha)-1=0. \tag{10}$$

The above definitions of the gauge surface and the gauge function are analogous to the corresponding well known notions of the yield function and the yield surface in the context of ideal-plasticity. Such discussion is made in Section 5, where the case of ideal-plasticity is considered separately.

Making use of the above definitions, we can redefine the stress triaxiality X_Σ in terms of $\bar{\boldsymbol{\Sigma}}$ as

$$X_\Sigma=\bar{\Sigma}_m/\bar{\Sigma}_{eq},\quad \bar{\Sigma}_{eq}=\sqrt{3\bar{\boldsymbol{\Sigma}}'\cdot\bar{\boldsymbol{\Sigma}}'/2},\quad \bar{\Sigma}_m=\bar{\Sigma}_{ii}/3, \tag{11}$$

where $\bar{\Sigma}_m$ and $\bar{\Sigma}_{eq}$ denote the mean and equivalent parts of $\bar{\boldsymbol{\Sigma}}$, respectively.

On the other hand, it follows from definitions (5) and (7) that

$$\bar{\boldsymbol{D}}=\dot{\varepsilon}_o\left(\frac{\Gamma_n(\bar{\boldsymbol{\sigma}};s_\alpha)}{\sigma_o}\right)^n\frac{\partial\Gamma_n(\bar{\boldsymbol{\sigma}};s_\alpha)}{\partial\bar{\boldsymbol{\sigma}}},\quad\text{or}\quad \bar{\boldsymbol{E}}=\frac{\bar{\boldsymbol{D}}}{\dot{\varepsilon}_o(\Gamma_n(\bar{\boldsymbol{\sigma}};s_\alpha)/\sigma_o)^n}, \tag{12}$$

where $\bar{\boldsymbol{E}}$ is a suitably normalized macroscopic strain-rate that is homogeneous of degree zero in $\bar{\boldsymbol{\sigma}}$. Note that the terms $\partial\Gamma_n/\partial\bar{\boldsymbol{\sigma}}$ and $\dot{\varepsilon}_o(\Gamma_n/\sigma_o)^n$ in (12) correspond to the direction and the magnitude, respectively, of $\bar{\boldsymbol{D}}$.

3. Variational estimates for the instantaneous effective behavior

In this section, we make use of the "second-order" method (*SOM*) of Ponte Castañeda (2002a) to estimate the effective stress potential $\tilde{U}$. This method is based on the construction of a "*linear comparison composite*" (LCC), with the same microstructure as the nonlinear composite, whose constituent phases are identified with appropriate linearizations of the given nonlinear phases resulting from a suitably designed variational principle. This allows the use of any available method to estimate the effective behavior of *linear* composites to generate corresponding estimates for *nonlinear* composites.

3.1. Linear Comparison Composite

For the class of porous materials considered in this work, the corresponding LCC is a viscous porous material, with a matrix phase characterized by a stress potential of the form (Ponte Castañeda, 2002a)

$$U_L(\boldsymbol{\sigma};\check{\boldsymbol{\sigma}},\mathbf{M})=U(\check{\boldsymbol{\sigma}})+\frac{\partial U}{\partial\boldsymbol{\sigma}}(\check{\boldsymbol{\sigma}})\cdot(\boldsymbol{\sigma}-\check{\boldsymbol{\sigma}})+\frac{1}{2}(\boldsymbol{\sigma}-\check{\boldsymbol{\sigma}})\cdot\mathbf{M}(\boldsymbol{\sigma}-\check{\boldsymbol{\sigma}}). \tag{13}$$

In this expression, $\check{\boldsymbol{\sigma}}$ is a uniform, reference stress tensor, which is taken to be *proportional* to the deviatoric macroscopic stress tensor $\bar{\boldsymbol{\sigma}}'$, letting the magnitude of this tensor to be defined later.

For viscoplastic composites, the following choice has been proposed by Ponte Castañeda (2002b) for the viscous compliance tensor $\mathbf{M}$ or, equivalently, for the modulus tensor $\mathbf{L}$ of the matrix phase in the LCC,

$$\mathbf{M}=\frac{1}{2\lambda}\mathbf{E}+\frac{1}{2\mu}\mathbf{F}+\frac{1}{3\kappa}\mathbf{J},\qquad \mathbf{L}=\mathbf{M}^{-1}=2\lambda\mathbf{E}+2\mu\mathbf{F}+3\kappa\mathbf{J}. \tag{14}$$

Here, λ and μ are shear viscous moduli to be defined later, and κ is the bulk viscosity of the matrix phase; the limit of incompressibility, i.e., $\kappa \to \infty$, will be considered later. For the above choice of $\check{\boldsymbol{\sigma}}$, the projection tensors $\mathbf{E}$ and $\mathbf{F}$ can be expressed as (Ponte Castañeda, 1996)

$$\mathbf{E} = \frac{3}{2}\bar{\boldsymbol{S}} \otimes \bar{\boldsymbol{S}}, \quad \mathbf{F} = \mathbf{K} - \mathbf{E}, \quad \mathbf{E} + \mathbf{F} + \mathbf{J} = \mathbf{I},$$
$$\mathbf{EE} = \mathbf{E}, \; \mathbf{FF} = \mathbf{F}, \; \mathbf{EF} = \mathbf{0}, \tag{15}$$

where

$$\bar{\boldsymbol{S}} = \frac{1}{\bar{\sigma}_{\mathrm{eq}}}\bar{\boldsymbol{\sigma}}' \tag{16}$$

and $\mathbf{I}$, $\mathbf{K}$ and $\mathbf{J}$ are the standard, fourth-order, identity, deviatoric and spherical projection tensors, respectively.

It should be emphasized that even though the nonlinear matrix phase is *isotropic*, the corresponding linearized phase in the LCC is, in general, *anisotropic*, in contrast with earlier methods, like the *VAR* method (Ponte Castañeda, 1991), where the corresponding LCC was *isotropic*. A measure of this anisotropy is given by the ratio

$$k = \frac{\lambda}{\mu}, \tag{17}$$

such that $k = 1$ and $k = 0$ correspond to an isotropic and strongly anisotropic linear matrix phase.

Using the appropriate specialization of the Levin (1967) relations for two-phase "thermoelastic" materials, we can write the effective potential of the LCC as (Talbot and Willis, 1992)

$$\tilde{U}_L(\bar{\boldsymbol{\sigma}}; \check{\boldsymbol{\sigma}}, \mathbf{M}) = (1-f)U(\check{\boldsymbol{\sigma}}) + \boldsymbol{\eta} \cdot \big(\bar{\boldsymbol{\sigma}} - (1-f)\check{\boldsymbol{\sigma}}\big) + \frac{1}{2}\bar{\boldsymbol{\sigma}} \cdot \tilde{\mathbf{M}}\bar{\boldsymbol{\sigma}} - \frac{1-f}{2}\check{\boldsymbol{\sigma}} \cdot \mathbf{M}\check{\boldsymbol{\sigma}}, \tag{18}$$

where $\tilde{\mathbf{M}}$ denotes the effective compliance tensor of the LCC and

$$\boldsymbol{\eta} = \frac{\partial U}{\partial \check{\boldsymbol{\sigma}}} - \mathbf{M}\check{\boldsymbol{\sigma}} = \frac{3\dot{\varepsilon}_o}{2\sigma_o}\left(\frac{\check{\sigma}_{\mathrm{eq}}}{\sigma_o}\right)^{n-1}\check{\boldsymbol{\sigma}} - \mathbf{M}\check{\boldsymbol{\sigma}}. \tag{19}$$

In this expression, use of (1) has been made for the computation of the term $\partial U/\partial \check{\boldsymbol{\sigma}}$.

To estimate $\tilde{\mathbf{M}}$, use is made of the Willis estimates (Willis, 1978; Ponte Castañeda and Willis, 1995), which are known to be quite accurate for particulate random systems like the ones of interest in this work, up to moderate concentrations of inclusions. For the above-mentioned class of porous materials, these estimates take the form

$$\tilde{\mathbf{M}} = \mathbf{M} + \frac{f}{1-f}\mathbf{Q}^{-1}. \tag{20}$$

In this expression, $\mathbf{Q}$ is a microstructural tensor, related to the Eshelby (1957) and Hill (1963) polarization tensor, which contains information about the shape and orientation of the voids and their distribution function, and is given by (Willis, 1978)

$$\mathbf{Q} = \frac{1}{4\pi \det(\boldsymbol{Z})}\int_{|\boldsymbol{\zeta}|=1}\big[\mathbf{L} - \mathbf{LH}(\boldsymbol{\zeta})\mathbf{L}\big]\big|\boldsymbol{Z}^{-1}\boldsymbol{\zeta}\big|^{-3} dS, \tag{21}$$

where $H_{(ij)(kl)} = (L_{iakb}\zeta_a\zeta_b)^{-1}\zeta_j\zeta_l|_{(ij)(kl)}$ (the parentheses denote symmetrization with respect to the corresponding indices), and $\boldsymbol{\zeta}$ is a unit vector. The symmetric second-order tensor $\boldsymbol{Z}$ characterizes the *instantaneous* shape and orientation of the inclusions and their distribution function, and can be expressed as (Willis, 1978)

$$\boldsymbol{Z} = w_1\mathbf{n}^{(1)} \otimes \mathbf{n}^{(1)} + w_2\mathbf{n}^{(2)} \otimes \mathbf{n}^{(2)} + \mathbf{n}^{(3)} \otimes \mathbf{n}^{(3)},$$
$$\det(\boldsymbol{Z}) = w_1 w_2. \tag{22}$$

Note that incompressibility of the nonlinear matrix phase requires the consideration of the incompressibility limit (i.e., $\kappa \to \infty$) in the kernel of the integral (21) but the resulting expressions are too cumbersome to be reported here. The final expression for $\tilde{\mathbf{M}}$ in relation (20) is compressible, since it corresponds to a porous material.

It should be emphasized that the above Willis estimates for $\tilde{\mathbf{M}}$ lead to uniform fields in the porous phase (Willis, 1978), which is consistent with the work of Eshelby (1957) in the dilute case. In fact, the above Willis estimates are exact for dilute composites. On the other hand, for non-dilute media, the fields within the voids are, in general, nonuniform, but this "nonuniformity" is negligible (Bornert et al., 1996) provided that the pores are not in close proximity to each other, i.e., their volume fraction is not so large compared to that of the matrix phase. This is an important observation we should bear in mind when the application of the Willis-type linear homogenization techniques is used for materials consisting of high concentrations of voids. Nevertheless, the focus of this work is on porous media with low to moderate concentrations of voids, and hence the Willis procedure is expected to be sufficiently accurate.

3.2. "Second-order" variational estimate

Once the LCC is specified, the *SOM* estimate for the effective stress potential of the nonlinear porous material is given by (Ponte Castañeda, 2002a; Idiart et al., 2006; Danas et al., 2008b)

$$\tilde{U}_{SOM}(\bar{\boldsymbol{\sigma}}) = \underset{\lambda,\mu}{\mathrm{stat}}\big\{\tilde{U}_L(\bar{\boldsymbol{\sigma}}; \check{\boldsymbol{\sigma}}, \lambda, \mu) + (1-f)V(\check{\boldsymbol{\sigma}}, \lambda, \mu)\big\}, \tag{23}$$

where $\tilde{U}_L$ is given by (18), and the "corrector" function V is defined as

$$V(\check{\boldsymbol{\sigma}}, \lambda, \mu) = \underset{\hat{\boldsymbol{\sigma}}}{\mathrm{stat}}\big[U(\hat{\boldsymbol{\sigma}}) - U_L(\hat{\boldsymbol{\sigma}}; \check{\boldsymbol{\sigma}}, \lambda, \mu)\big]. \tag{24}$$

The stationary operation (stat) consists in setting the partial derivative of the argument with respect to the appropriate variables equal to zero, which yields a set of nonlinear equations for the variables λ, μ and $\hat{\boldsymbol{\sigma}}$, as shown next.

Making use of the special form (14) of the tensor $\mathbf{M}$ (in the limit $\kappa \to \infty$), we can define two components of the tensor $\hat{\boldsymbol{\sigma}}$ that are "parallel" and "perpendicular" to the corresponding reference tensor $\check{\boldsymbol{\sigma}}$, respectively, i.e., $\hat{\sigma}_\parallel = (\frac{3}{2}\hat{\boldsymbol{\sigma}} \cdot \mathbf{E}\hat{\boldsymbol{\sigma}})^{1/2}$ and $\hat{\sigma}_\perp = (\frac{3}{2}\hat{\boldsymbol{\sigma}} \cdot \mathbf{F}\hat{\boldsymbol{\sigma}})^{1/2}$, such that the equivalent part of the tensor $\hat{\boldsymbol{\sigma}}$ reduces to

$$\hat{\sigma}_{\mathrm{eq}} = \sqrt{\hat{\sigma}_\parallel^2 + \hat{\sigma}_\perp^2}. \tag{25}$$

It is noted that the quantities $\hat{\sigma}_{\mathrm{eq}}$, $\hat{\sigma}_\parallel$ and $\hat{\sigma}_\perp$ turn out to depend on certain traces—specified by the projection tensors $\mathbf{E}$ and $\mathbf{F}$—of the fluctuations of the stress field in the LCC (Ponte Castañeda, 2002a; Idiart and Ponte Castañeda, 2005; Danas et al., 2008a, 2008b).

It follows from the above definitions that the stationarity operation in (24) leads to two equations for the moduli λ and μ, which read

$$\dot{\varepsilon}_o\left(\frac{\hat{\sigma}_{\mathrm{eq}}}{\sigma_o}\right)^n\frac{\hat{\sigma}_\parallel}{\hat{\sigma}_{\mathrm{eq}}} - \dot{\varepsilon}_o\left(\frac{\check{\sigma}_{\mathrm{eq}}}{\sigma_o}\right)^n = \frac{1}{3\lambda}(\hat{\sigma}_\parallel - \check{\sigma}_{\mathrm{eq}}),$$
$$\dot{\varepsilon}_o\left(\frac{\hat{\sigma}_{\mathrm{eq}}}{\sigma_o}\right)^{n-1} = \frac{\sigma_o}{3\mu}. \tag{26}$$

These two relations can then be combined into the single equation

$$k\left(\frac{\hat{\sigma}_{\mathrm{eq}}}{\check{\sigma}_{\mathrm{eq}}}\right)^{1-n} = (k-1)\frac{\hat{\sigma}_\parallel}{\check{\sigma}_{\mathrm{eq}}} + 1, \tag{27}$$

where k is the ratio defined by (17).

The scalar quantities $\hat{\sigma}_\parallel$ and $\hat{\sigma}_\perp$ are positively homogeneous functions of degree one of the applied macroscopic loading $\bar{\boldsymbol{\sigma}}$, and result from the stationarity conditions in relation (23) with respect to λ and μ (Ponte Castañeda, 2002a; Idiart et al., 2006; Danas et al., 2008b), such that

$$\hat{\sigma}_{\parallel} = \check{\sigma}_{\text{eq}} + \sqrt{\check{\sigma}_{\text{eq}}^2 + \frac{\bar{\sigma}_{\text{eq}}^2}{1-f} - \frac{2\check{\sigma}_{\text{eq}}\bar{\sigma}_{\text{eq}}}{1-f} + \frac{3f}{(1-f)^2}\bar{\boldsymbol{\sigma}} \cdot \frac{\partial \mathbf{Q}^{-1}}{\partial \lambda^{-1}}\bar{\boldsymbol{\sigma}}},$$
$$\hat{\sigma}_{\perp} = \frac{\sqrt{3f}}{1-f}\sqrt{\bar{\boldsymbol{\sigma}} \cdot \frac{\partial \mathbf{Q}^{-1}}{\partial \mu^{-1}}\bar{\boldsymbol{\sigma}}}, \tag{28}$$

where use of relations (18)–(20) has been made. It is further noted that $\hat{\sigma}_{\parallel}$ and $\hat{\sigma}_{\perp}$ are homogeneous functions of degree zero in $\mathbf{M}$, and therefore, depend on the moduli λ and μ only through the anisotropy ratio k. Introducing expressions (28) for $\hat{\sigma}_{\parallel}$ and $\hat{\sigma}_{\perp}$ into (27), we obtain a single algebraic, nonlinear equation for k, which must be solved numerically for a given choice of the reference tensor $\check{\boldsymbol{\sigma}}$.

Finally, making use of relations (27) and (28), the estimate (23) for the effective stress potential of the nonlinear porous composite can be simplified to

$$\tilde{U}_{SOM}(\bar{\boldsymbol{\sigma}}) = (1-f)\left[\frac{\dot{\varepsilon}_o\sigma_o}{1+n}\left(\frac{\hat{\sigma}_{\text{eq}}}{\sigma_o}\right)^{n+1} - \dot{\varepsilon}_o\left(\frac{\check{\sigma}_{\text{eq}}}{\sigma_o}\right)^n\left(\hat{\sigma}_{\parallel} - \frac{\bar{\sigma}_{\text{eq}}}{(1-f)}\right)\right], \tag{29}$$

where the tensor $\check{\boldsymbol{\sigma}}$ remains to be specified.

The gauge factor Γ_n^{som} associated with the *SOM* can be derived by equating (7) with (29), such that

$$\Gamma_n^{\text{som}}(\bar{\boldsymbol{\sigma}}) = (1-f)^{\frac{1}{1+n}}\hat{\sigma}_{\text{eq}}\left[1-(1+n)\left(\frac{\check{\sigma}_{\text{eq}}}{\hat{\sigma}_{\text{eq}}}\right)^n \times\left(\frac{\hat{\sigma}_{\parallel}}{\hat{\sigma}_{\text{eq}}} - \frac{\bar{\sigma}_{\text{eq}}}{(1-f)\hat{\sigma}_{\text{eq}}}\right)\right]^{\frac{1}{1+n}}. \tag{30}$$

It should be remarked at this point that the earlier *VAR* method of Ponte Castañeda (1991) can be formally obtained by letting $\check{\sigma}_{\text{eq}}$ tend to zero in (29). This would further imply that the anisotropy ratio becomes $k=1$ in this case (by setting $\check{\sigma}_{\text{eq}}=0$ in (26)), i.e., the LCC becomes isotropic with $\lambda=\mu$. Furthermore, note that the corresponding gauge factor Γ_n^{var} associated with the *VAR* method is simply given by $\Gamma_n^{\text{var}}(\bar{\boldsymbol{\sigma}}) = (1-f)^{\frac{1}{1+n}}\hat{\sigma}_{\text{eq}}$.

The corresponding macroscopic stress–strain-rate relation then follows by differentiation of (23) or, equivalently, (29). The resulting expression can be shown to reduce to (Idiart and Ponte Castañeda, 2007; Danas et al., 2008b)

$$\bar{D}_{ij} = (\bar{D}_L)_{ij} + (1-f)g_{mn}\frac{\partial\check{\sigma}_{mn}}{\partial\bar{\sigma}_{ij}}, \qquad (\bar{D}_L)_{ij} = \tilde{M}_{ijkl}\bar{\sigma}_{kl} + \eta_{ij}, \tag{31}$$

where $\bar{\boldsymbol{D}}_L$ denotes the macroscopic strain-rate in the LCC, and the second-order tensor $\boldsymbol{g}$ is given by

$$g_{ij} = \left(\frac{1}{2\lambda} - \frac{1}{2\lambda_t}\right)\left(\hat{\sigma}_{\parallel} - \frac{\bar{\sigma}_{\text{eq}}}{(1-f)}\right)\frac{\check{\sigma}_{ij}}{\check{\sigma}_{\text{eq}}} + \frac{f}{2(1-f)^2}\bar{\sigma}_{kl}\frac{\partial[Q(\check{\boldsymbol{\sigma}})]^{-1}_{klmn}}{\partial\check{\sigma}_{ij}}\bigg|_{\lambda,\mu}\bar{\sigma}_{mn}, \tag{32}$$

with $\lambda_t = \sigma_o/(3\dot{\varepsilon}_o n)(\check{\sigma}_{\text{eq}}/\sigma_o)^{1-n}$. Finally, it is worth noting that, in (31), the strain-rate in the nonlinear porous material $\bar{\boldsymbol{D}}$ is not equal to the average strain-rate $\bar{\boldsymbol{D}}_L$ in the LCC.

3.3. *Choices for the reference stress tensor*

The estimate (29) requires a prescription for the reference stress tensor $\check{\boldsymbol{\sigma}}$. Recently, Danas et al. (2008a, 2008b) suggested a prescription for $\check{\boldsymbol{\sigma}}$ in the context of isotropic and transversely isotropic porous media. The advantage of that prescription lies in the fact that in the limiting case of spherical or cylindrical with circular cross-section pores subjected to purely hydrostatic loading, the resulting *SOM* estimates recover the exact result for the composite sphere or cylinder assemblage microstructures (CSA or CCA). The CSA and CCA microstructures constitute commonly used models for isotropic and transversely isotropic porous materials, respectively, and the reason for this is linked to the fact that the effective response of such composites is known exactly (Hashin, 1962; Gurson, 1977; Leblond et al., 1994) in closed form in the special case of hydrostatic loading.

In contrast, there exist no analytical closed-form solution for the analogous problem of ellipsoidal particulate microstructures, although in certain special cases, such as for a confocal, spheroidal shell subjected to a specific axisymmetric loading (Gologanu et al., 1993, 1994), it is possible to develop analytical solutions. On the other hand, the *VAR* method of Ponte Castañeda (1991), which is capable of providing estimates (bounds) for the effective response of a porous material consisting of ellipsoidal voids subjected to general loading conditions, is known to be overly stiff, particularly for isotropic porous materials and high triaxiality loadings. In view of the above observations and the work of Danas et al. (2008a, 2008b), an *ad-hoc* prescription for $\check{\boldsymbol{\sigma}}$ is proposed in the following paragraphs, in such a way that the resulting *SOM* estimates recover the exact result for CSA and CCA microstructures in the purely hydrostatic limit, while remaining sufficiently accurate for arbitrary ellipsoidal microstructures.

Before proceeding to a specific prescription, it is necessary to note that, in the special case of purely hydrostatic loading (i.e., $|X_\Sigma| \to \infty$), the effective stress potential $\tilde{U}$ of a porous medium with an isotropic matrix does not depend on the orientation vectors $\mathbf{n}^{(i)}$ $(i=1,2,3)$, i.e., $\tilde{U}(\bar{\sigma}_m; f, w_1, w_2, \mathbf{n}^{(i)}) = \tilde{U}(\bar{\sigma}_m; f, w_1, w_2)$. Consequently, any estimate for $\tilde{U}$ should reduce to the following analytical results itemized below:

1. if $w_1 = w_2 = 1$, $\tilde{U}$ should recover the analytical result delivered when a spherical cavity (or CSA) is subjected to purely hydrostatic loading.
2. if $w_1 = w_2 \to \infty$ or $w_1 = 1$ and $w_2 \to \infty$ or $w_1 \to \infty$ and $w_2 = 1$, $\tilde{U}$ should recover the analytical result obtained when a cylindrical shell (or CCA) is subjected to purely hydrostatic loading.

Thus, for purely hydrostatic loading, $\tilde{U}$ reduces to

$$\tilde{U}_H(\bar{\boldsymbol{\sigma}}; f, w_1, w_2) = \frac{\dot{\varepsilon}_o\tilde{\sigma}_w}{1+n}\left(\frac{3}{2}\frac{|\bar{\sigma}_m|}{\tilde{\sigma}_w}\right)^{1+n}, \tag{33}$$

where $\tilde{\sigma}_w$ (the subscript w is used to emphasize the dependence on the aspect ratios w_1 and w_2) denotes the effective flow stress of the porous medium. In this last expression, use has been made of the fact that the effective stress potential $\tilde{U}$ is homogeneous of degree $n+1$ in $\bar{\boldsymbol{\sigma}}$, whereas the form (33) implies that the estimation of $\tilde{\sigma}_w$ determines fully the effective behavior of the porous material in the hydrostatic limit.

In this connection, when a CSA and CCA is subjected to hydrostatic loading conditions (i.e., $|X_\Sigma| \to \infty$), the corresponding effective flow stress can be computed exactly by solving the isolated spherical or cylindrical shell problem, and is given by (Michel and Suquet, 1992)

$$\frac{\tilde{\sigma}_{w=1}}{\sigma_o} = n\left(f^{-1/n} - 1\right) \quad \text{and} \quad \frac{\tilde{\sigma}_{w\to\infty}}{\sigma_o} = \left(\frac{\sqrt{3}}{2}\right)^{\frac{1+n}{n}}\frac{\tilde{\sigma}_{w=1}}{\sigma_o}, \tag{34}$$

where $\tilde{\sigma}_{w=1}$ and $\tilde{\sigma}_{w\to\infty}$ are the effective flow stresses of the spherical and the cylindrical shells, respectively.

On the other hand, the corresponding effective flow stresses delivered by the *VAR* procedure (denoted with the subscript "*var*"), for porous media containing spherical (denoted with $w = 1$) and cylindrical (denoted with $w \to \infty$) voids subjected to purely hydrostatic loading, read

$$\frac{\tilde{\sigma}^{\rm var}_{w=1}}{\sigma_o} = \frac{1-f}{\sqrt{f^{\frac{1+n}{n}}}} \quad \text{and} \quad \frac{\tilde{\sigma}^{\rm var}_{w\to\infty}}{\sigma_o} = \left(\frac{\sqrt{3}}{2}\right)^{\frac{1+n}{n}} \frac{\tilde{\sigma}^{\rm var}_{w=1}}{\sigma_o}. \tag{35}$$

Clearly, the estimates (34) and (35) deviate significantly at low porosities and high nonlinearities, whereas they coincide for linear porous media (i.e., $n = 1$).

By contrast, it should be emphasized that there exist no exact solutions for the effective flow stress $\tilde{\sigma}_w$ of a porous material with ellipsoidal voids of arbitrary shape. However, it is interesting to note that the effective flow stresses delivered by the shell problem and the *VAR* method satisfy the following *non-trivial* relation

$$\frac{\tilde{\sigma}_{w\to\infty}}{\tilde{\sigma}^{\rm var}_{w\to\infty}} = \frac{\tilde{\sigma}_{w=1}}{\tilde{\sigma}^{\rm var}_{w=1}}, \quad \text{or} \quad \tilde{\sigma}_{w\to\infty} = \frac{\tilde{\sigma}_{w=1}}{\tilde{\sigma}^{\rm var}_{w=1}} \tilde{\sigma}^{\rm var}_{w\to\infty}. \tag{36}$$

Making use now of result (36) and due to lack of an analytical estimate in the case of general ellipsoidal microstructures, we approximate the effective flow stress $\tilde{\sigma}_w$, associated with arbitrary aspect ratios w_1 and w_2, by

$$\frac{\tilde{\sigma}_w}{\tilde{\sigma}^{\rm var}_w} = \frac{\tilde{\sigma}_{w=1}}{\tilde{\sigma}^{\rm var}_{w=1}} = \frac{\tilde{\sigma}_{w\to\infty}}{\tilde{\sigma}^{\rm var}_{w\to\infty}}, \quad \text{or} \quad \tilde{\sigma}_w = \frac{\tilde{\sigma}_{w=1}}{\tilde{\sigma}^{\rm var}_{w=1}} \tilde{\sigma}^{\rm var}_w = \frac{\tilde{\sigma}_{w\to\infty}}{\tilde{\sigma}^{\rm var}_{w\to\infty}} \tilde{\sigma}^{\rm var}_w, \tag{37}$$

where $\tilde{\sigma}^{\rm var}_w$ is the corresponding effective flow stress delivered by the *VAR* procedure for any value of w_1 and w_2, determined by (Ponte Castañeda, 1991; Willis, 1991; Michel and Suquet, 1992; Danas, 2008)

$$\left(\frac{\tilde{\sigma}^{\rm var}_w}{\sigma_o}\right)^{-n} = (1-f)\left[\frac{4\boldsymbol{\delta}\cdot\widehat{\mathbf{M}}\boldsymbol{\delta}}{3(1-f)}\right]^{\frac{n+1}{2}}, \quad \text{with } \widehat{\mathbf{M}} = \tilde{\mathbf{M}}|_{\mu=1,\ k=1}, \tag{38}$$

with $\boldsymbol{\delta}$ denoting the second-order identity tensor and $\tilde{\mathbf{M}}$ given by (20).

The main advantage of prescription (37) is that the estimate for $\tilde{U}$ recovers automatically the two conditions described previously. On the other hand, it should be noted that when the porous material tends to a porous laminate or porous "sandwich" (for instance, $w_1 = w_2 \to 0$ with f finite), the *VAR* estimate can be shown to be exact, i.e., the effective flow stress $\tilde{\sigma}^{\rm var}_w$ for such a microstructure is identically zero. This implies that $(37)_1$ is not exact in this case, in the sense that the ratio $\tilde{\sigma}_w/\tilde{\sigma}^{\rm var}_w$ should go to unity. However, it follows from $(37)_2$ that the absolute value for $\tilde{\sigma}_w$ is zero and hence equal to the exact value. In this regard, the absolute error introduced by (37) for the determination of $\tilde{\sigma}_w$ in this extreme case of a porous laminate is expected to be rather small.

Given the estimate (37) for the effective behavior of a porous material containing ellipsoidal voids subjected to purely hydrostatic loading, we adopt an ad-hoc prescription for the reference stress tensor, given by (Danas et al., 2008b)

$$\check{\boldsymbol{\sigma}} = \xi(X_\Sigma, \bar{\boldsymbol{S}}, s_\alpha, n)\bar{\boldsymbol{\sigma}}', \tag{39}$$

where $\bar{\boldsymbol{S}}$ is defined by (16), s_α denotes the set of the microstructural variables (see (2)), n is the nonlinear exponent of the matrix phase, and

$$\xi(X_\Sigma, \bar{\boldsymbol{S}}; s_\alpha, n) = \frac{1-\beta_1(X_\Sigma, f)f}{1-f} + \alpha_m(\bar{\boldsymbol{S}})|X_\Sigma|\left(\exp\left[-\frac{\alpha_{\rm eq}(\bar{\boldsymbol{S}})}{|X_\Sigma|}\right] + \beta_2(f,n)\frac{X_\Sigma^4}{1+X_\Sigma^4}\right), \tag{40}$$

is a suitably chosen interpolation function which is homogeneous of degree zero in $\bar{\boldsymbol{\sigma}}$. The coefficients β_1 and β_2 are prescribed in an *ad-hoc* manner to ensure the convexity of the effective stress potential $\tilde{U}_{\rm som}$ and are detailed in Appendix A. The coefficients α_m and $\alpha_{\rm eq}$ are, in general, functions of the microstructural variables s_α, the nonlinearity n of the matrix, the stress tensor $\bar{\boldsymbol{S}}$, but not of the stress triaxiality X_Σ.

The coefficient α_m is computed such that the estimate for the effective stress potential $\tilde{U}_{\rm som}$, delivered by the *SOM* method in relation (29), coincides with the approximate solution for $\tilde{U}$ in relation (33) (with the use of (37)) in the hydrostatic limit. This condition may be written schematically as

$$\tilde{U}_{\rm som} \to \tilde{U}_H \quad \text{as } |X_\Sigma| \to \infty \quad \Rightarrow \quad \alpha_m = \alpha_m(\bar{\boldsymbol{S}}, s_\alpha, n), \tag{41}$$

which yields a nonlinear algebraic equation for α_m.

On the other hand, computation of the coefficient $\alpha_{\rm eq}$ requires an appropriate estimate for the deviatoric part of the normalized strain-rate $\bar{\boldsymbol{E}}'$ (the prime denotes the deviatoric part), defined in (12), in the limit as $X_\Sigma \to \pm\infty$. In this regard, we first note that, in general, there exists no exact result for $\bar{\boldsymbol{E}}'$, except for the special cases of spherical or cylindrical with circular cross-section voids and porous sandwiches, where $\bar{\boldsymbol{E}}' = \mathbf{0}$ as $X_\Sigma \to \pm\infty$. This result is exact for finite nonlinearities, i.e., $1 < n < \infty$, while the special case of ideal plasticity will be considered in a separate section later. On the other hand, the corresponding *VAR* estimate recovers these exact solutions, i.e., $\bar{\boldsymbol{E}}'_{\rm var} = \mathbf{0}$ as $X_\Sigma \to \pm\infty$ for porous media with spherical or cylindrical with circular cross-section voids, as well as for porous sandwiches.

In view of this and due to absence of any other information regarding the computation of $\bar{\boldsymbol{E}}'$ in the hydrostatic limit, the following prescription is adopted for $\bar{\boldsymbol{E}}'_{\rm som}$, and consequently for $\alpha_{\rm eq}$:

$$\bar{\boldsymbol{E}}'_{\rm som} \to \bar{\boldsymbol{E}}'_{\rm var} \quad \text{as } X_\Sigma \to \pm\infty \quad \Rightarrow \quad \alpha_{\rm eq} = \alpha_{\rm eq}(\bar{\boldsymbol{S}}, s_\alpha, n) \quad \forall w_1, w_2, \mathbf{n}^{(i)}. \tag{42}$$

In this last relation, $\bar{\boldsymbol{E}}'_{\rm var}$ is given by (Ponte Castañeda, 1991; Danas, 2008)

$$\bar{\boldsymbol{E}}'_{\rm var} = 3\,\mathrm{sgn}(X_\Sigma)\left(\bar{\Sigma}^H_m\big|_{\rm var}\right)^n\left(\frac{3\boldsymbol{\delta}\cdot\widehat{\mathbf{M}}\boldsymbol{\delta}}{1-f}\right)^{\frac{n-1}{2}}\mathbf{K}\widehat{\mathbf{M}}\boldsymbol{\delta},$$
$$\bar{\Sigma}^H_m\big|_{\rm var} = \frac{2}{3}\left(\frac{\tilde{\sigma}^{\rm var}_w}{\sigma_o}\right)^{\frac{n}{n+1}}, \tag{43}$$

for any value of w_1 and w_2 in the limit as $X_\Sigma \to \pm\infty$. Moreover, $\widehat{\mathbf{M}}$ is given by (38), whereas $\bar{\Sigma}^H_m|_{\rm var}$ is a normalized hydrostatic stress detailed in Appendix B. The physical interpretation of condition (42) is that the slope of the *SOM* gauge curve is identical to the slope of the corresponding *VAR* gauge curve in the hydrostatic limit. In addition, it should be emphasized that condition (42) implies that $\alpha_{\rm eq}$ does not depend on the magnitude of the macroscopic stress tensor $\bar{\boldsymbol{\sigma}}$, which is a requirement of definition (39) and (40). This is a direct consequence of the fact that the terms $\bar{\boldsymbol{E}}'_{\rm som}$ and $\bar{\boldsymbol{E}}'_{\rm var}$ are homogeneous of degree zero in $\bar{\boldsymbol{\sigma}}$.

While the computation of the coefficient α_m in (41) needs to be performed numerically, the evaluation of $\alpha_{\rm eq}$ can be further simplified to the analytical expression

$$\alpha_{\rm eq} = \alpha_m^{-1}\left[1 + \frac{\frac{3}{2}\check{\sigma}_{\rm eq}(\bar{\boldsymbol{\Sigma}})^n - \check{\sigma}_{\rm eq}(\bar{\boldsymbol{\Sigma}})(2\bar{\lambda})^{-1} + \bar{d}_\parallel - \bar{d}_{\rm var}}{(1-f)\hat{\sigma}_\parallel(\bar{\boldsymbol{\Sigma}})} \times \left(\frac{1}{2\bar{\lambda}} - \frac{1}{2\bar{\lambda}_t}\right)^{-1}\right]. \tag{44}$$

Here, use has been made of definition (9) for the normalized macroscopic stress tensor $\bar{\boldsymbol{\Sigma}}$, as well as of the fact that $\check{\sigma}_{\rm eq}$, $\hat{\sigma}_\parallel$ and $\hat{\sigma}_{\rm eq}$ are homogeneous functions of degree one in $\bar{\boldsymbol{\sigma}}$. It is further emphasized that all the quantities involved in the above relation must be evaluated in the hydrostatic limit $X_\Sigma \to \pm\infty$, i.e., for

$$\bar{\boldsymbol{\Sigma}} = \mathrm{sgn}(X_\Sigma)\,\bar{\Sigma}^H_m\big|_{\rm som}\boldsymbol{\delta}, \qquad \bar{\Sigma}^H_m\big|_{\rm som} = \frac{2}{3}\left(\frac{\tilde{\sigma}_w}{\sigma_o}\right)^{\frac{n}{n+1}}, \tag{45}$$

where $\tilde{\sigma}_w$ is given by (37) and $\bar{\Sigma}_m^H|_{som}$ denotes the corresponding normalized hydrostatic stress obtained by the *SOM* (see Appendix B). Then, the terms in (44) associated with the *SOM* method are given by

$$\bar{\lambda} = k^H \bar{\mu}, \quad \bar{\mu} = \hat{\sigma}_{eq}(\bar{\boldsymbol{\Sigma}})^{1-n}/3, \quad \bar{\lambda}_t = \frac{1}{3n}\check{\sigma}_{eq}(\bar{\boldsymbol{\Sigma}})^{1-n},$$

$$\bar{d}_{\parallel} = \frac{3}{2}\,\mathrm{sgn}(X_\Sigma)\bar{\Sigma}_m^H\big|_{som}\bar{\mathbf{S}}\cdot\tilde{\mathbf{M}}|_{k^H,\bar{\mu}}\boldsymbol{\delta},$$

with $\tilde{\mathbf{M}}$ defined by (20). Furthermore, for the computation of k^H in (46), it is necessary to solve the nonlinear equation (27) for the anisotropy ratio k in the hydrostatic limit. On the other hand, the term $\bar{d}_{var}$ in (44), associated with the *VAR* method, is given by

$$\bar{d}_{var} = \frac{9}{2}\,\mathrm{sgn}(X_\Sigma)\big(\bar{\Sigma}_m^H\big|_{var}\big)^n\left(\frac{3\boldsymbol{\delta}\cdot\widehat{\mathbf{M}}\boldsymbol{\delta}}{1-f}\right)^{\frac{n-1}{2}}\bar{\mathbf{S}}\cdot\widehat{\mathbf{M}}\boldsymbol{\delta},$$

with $\widehat{\mathbf{M}}$ and $\bar{\Sigma}_m^H|_{var}$ defined in (38) and (43), respectively.

At this point, several observations are in order. First, the choice (39) guarantees that the resulting effective stress potential (29) is a homogeneous function of degree $n+1$ in the average stress $\bar{\boldsymbol{\sigma}}$ for all triaxialities X_Σ, as it should. Second, it is noted that the choice (39) reduces to $\check{\boldsymbol{\sigma}} = \bar{\boldsymbol{\sigma}}'$ for $X_\Sigma = 0$, which is precisely the prescription earlier proposed by Idiart and Ponte Castañeda (2005) (see also Idiart et al., 2006) for general loadings. This prescription has been found to deliver accurate estimates when the porous medium is subjected to isochoric loadings, but reduces to zero for purely hydrostatic loadings and therefore coincides with the *VAR* estimates in this limit (Danas et al., 2008a). Third, because the new prescription (39) is nonzero for purely hydrostatic loading, the matrix phase in the LCC remains anisotropic in this limit, in contrast with the earlier choice, $\check{\boldsymbol{\sigma}} = \bar{\boldsymbol{\sigma}}'$, which leads to an isotropic LCC. Finally, the above prescription for the reference stress tensor reduces to the one provided by Danas et al. (2008a, 2008b) for isotropic and transversely isotropic porous media.

In summary, relation (39), together with relations (41) and (42) (or (44)), completely define the reference stress tensor $\check{\boldsymbol{\sigma}}$, and thus, result (29) can be used to estimate the instantaneous effective behavior of the viscoplastic porous material.

3.4. Phase average fields

In this subsection, the focus is on estimating the average stress, strain-rate and spin in each phase of the porous material. This is necessary for the prediction of the evolution of the microstructural variables s_α to be discussed in the next section. Because of the presence of the vacuous phase the phase average stress tensors in the LCC and the nonlinear material are trivially given by

$$(1-f)\bar{\boldsymbol{\sigma}}^{(1)} = \bar{\boldsymbol{\sigma}} = (1-f)\bar{\boldsymbol{\sigma}}_L^{(1)} = \bar{\boldsymbol{\sigma}}_L, \qquad \bar{\boldsymbol{\sigma}}^{(2)} = \bar{\boldsymbol{\sigma}}_L^{(2)} = \mathbf{0}, \tag{46}$$

where the subscript L serves to denote quantities in the LCC, whereas label 1 and 2 refer to the matrix and vacuous phase, respectively.

The estimation of the average strain-rate and spin in each phase is more complicated. Recall first that, regardless of any prescription for the estimation of the average strain-rate and spin in each phase, the following relations for the macroscopic and the phase average quantities must always hold, both in the nonlinear composite and the LCC

$$\bar{\boldsymbol{D}} = (1-f)\bar{\boldsymbol{D}}^{(1)} + f\bar{\boldsymbol{D}}^{(2)}, \qquad \bar{\boldsymbol{D}}_L = (1-f)\bar{\boldsymbol{D}}_L^{(1)} + f\bar{\boldsymbol{D}}_L^{(2)}, \tag{47}$$

and

$$\bar{\boldsymbol{\Omega}} = (1-f)\bar{\boldsymbol{\Omega}}^{(1)} + f\bar{\boldsymbol{\Omega}}^{(2)}, \qquad \bar{\boldsymbol{\Omega}}_L = (1-f)\bar{\boldsymbol{\Omega}}_L^{(1)} + f\bar{\boldsymbol{\Omega}}_L^{(2)}, \tag{48}$$

with $\bar{\boldsymbol{\Omega}}$ and $\bar{\boldsymbol{\Omega}}_L$ denoting the macroscopic spin in the nonlinear and LCC, respectively. The macroscopic spin is applied externally in the problem, which implies that $\bar{\boldsymbol{\Omega}} = \bar{\boldsymbol{\Omega}}_L$. In the following, the discussion will be focused on the calculation of the average strain-rate $\bar{\boldsymbol{D}}^{(2)}$ and spin $\bar{\boldsymbol{\Omega}}^{(2)}$ in the vacuous phase; the corresponding quantities $\bar{\boldsymbol{D}}^{(1)}$ and $\bar{\boldsymbol{\Omega}}^{(1)}$ for the matrix phase are then determined from (47) and (48) for given macroscopic $\bar{\boldsymbol{D}}$ and $\bar{\boldsymbol{\Omega}}$.

Making use of the identities (47) and the incompressibility of the matrix phase, the hydrostatic part of the macroscopic strain-rate $\bar{D}_m = \bar{D}_{ii}/3$, and the average strain-rate in the voids, $\bar{D}_m^{(2)}$, are related through

$$\bar{D}_m^{(2)} = \frac{1}{f}\bar{D}_m, \quad \text{and} \quad \bar{D}_m^{(1)} = 0. \tag{49}$$

It is easy to verify that $\bar{D}_m^{(2)}$ cannot be equal to $(\bar{D}_m^{(2)})_L$ since $\bar{D}_m \neq (\bar{D}_m)_L$ in (31). The result (49) is exact and no approximations are involved, apart from those intrinsic to the calculation of $\bar{D}_m$ by (31).

The computation of the deviatoric part of the average strain-rate, $\bar{\boldsymbol{D}}^{(2)\prime}$, in the vacuous phase is nontrivial. In the work of Idiart and Ponte Castañeda (2007), the idea of computing $\bar{\boldsymbol{D}}^{(2)}$ lies in perturbing the local nonlinear phase stress potential U, given by (1), with respect to a constant polarization type field $\boldsymbol{p}$, solving the perturbed problem through the homogenization procedure and then considering the derivative with respect to $\boldsymbol{p}$, while letting it go to zero. Consequently, the expression for the average strain-rate in the vacuous phase can be shown to be of the form (Idiart and Ponte Castañeda, 2007)

$$\bar{\boldsymbol{D}}^{(2)} = \bar{\boldsymbol{D}}_L^{(2)} - \frac{1-f}{f}\boldsymbol{g}\frac{\partial\check{\boldsymbol{\sigma}}}{\partial\boldsymbol{p}}\bigg|_{\boldsymbol{p}\to\mathbf{0}}, \tag{50}$$

with $\boldsymbol{g}$ given by (32). Also $\bar{\boldsymbol{D}}_L^{(2)}$ can be shown to reduce to (Ponte Castañeda, 2006; Danas, 2008)

$$\bar{\boldsymbol{D}}_L^{(2)} = \frac{1}{f}(\tilde{\mathbf{M}} - \mathbf{M})\bar{\boldsymbol{\sigma}} + \boldsymbol{\eta} = \frac{1}{1-f}\mathbf{Q}^{-1}\bar{\boldsymbol{\sigma}} + \boldsymbol{\eta}, \tag{51}$$

with $\mathbf{Q}$ and $\boldsymbol{\eta}$ given by (21) and (19), respectively.

Relation (50) necessitates the evaluation of the term $\partial\check{\boldsymbol{\sigma}}/\partial\boldsymbol{p}$ or equivalently the variation of $\check{\boldsymbol{\sigma}}$ with respect to the perturbation parameter $\boldsymbol{p}$, which, in turn, requires the computation of the effective stress potential of a perturbed shell problem. The solution of the shell problem assuming a perturbed nonlinear potential law for the matrix phase is too complicated and probably can be achieved only by numerical calculations for general ellipsoidal microstructures. Another option is to evaluate the deviatoric part of $\bar{\boldsymbol{D}}^{(2)}$ approximately, while the hydrostatic part of $\bar{\boldsymbol{D}}^{(2)}$ is obtained by relation (49) exactly within the approximation intrinsic to the method. In this regard, we set

$$\bar{\boldsymbol{D}}^{(2)\prime} = \bar{\boldsymbol{D}}_L^{(2)\prime} \quad \Rightarrow \quad \bar{\boldsymbol{D}}^{(2)} = \frac{1}{f}\bar{D}_m\boldsymbol{\delta} + \bar{\boldsymbol{D}}_L^{(2)\prime}, \tag{52}$$

and attempt to estimate the resulting error introduced by ignoring the second term in (50). For this analysis, it is important to mention that the reference stress tensor $\check{\boldsymbol{\sigma}}$ prescribed in relation (39) could depend on $\boldsymbol{p}$ only through the coefficients α_m and α_{eq}. This implies that relation (52) is exact in the low triaxiality limit $X_\Sigma = 0$, since, in this case, $\check{\boldsymbol{\sigma}} = \bar{\boldsymbol{\sigma}}'$ and hence does not depend on $\boldsymbol{p}$ by definition. Under this observation, it is expected that prescription (52) is sufficiently accurate for low triaxiality loadings.

In contrast, at high triaxiality loadings the error is expected to be maximum. Estimating this error is possible only in special cases. In particular, in the cases of isotropic and transversely isotropic porous media that are subjected to purely hydrostatic loading, the exact result reads $\bar{\boldsymbol{D}}^{(2)\prime} = \mathbf{0}$. It can be verified that in those cases use of relation (52) introduces an error less than 1% in the computation of the deviatoric part of $\bar{\boldsymbol{D}}^{(2)}$ for small and moderate porosities. Furthermore, in this high triaxiality regime, it is expected (it will be verified in Part II of this work) that the hydrostatic part of $\bar{\boldsymbol{D}}$, i.e., $\bar{D}_m^{(2)}$, is predominant and controls the effective behavior of the porous material. Therefore, evaluation of the average strain-rate in the voids from relation (52) is expected to be sufficiently *accurate* and *simple* for the purposes of this work.

Following a similar line of thought, and due to lack of results for the estimation of the phase average spin of nonlinear materials, the assumption will be made here that the average spin in the vacuous phase $\bar{\boldsymbol{\Omega}}^{(2)}$ of the nonlinear porous material can be approximated by the average spin in the vacuous phase of the LCC, $\bar{\boldsymbol{\Omega}}_L^{(2)}$. This approximation becomes (Ponte Castañeda, 2006; Danas, 2008)

$$\bar{\boldsymbol{\Omega}}^{(2)} = \bar{\boldsymbol{\Omega}}_L^{(2)} = \bar{\boldsymbol{\Omega}} + \boldsymbol{\Pi}\mathbf{L}\mathbf{Q}^{-1}\bar{\boldsymbol{\sigma}},$$
$$\boldsymbol{\Pi} = \frac{1}{4\pi \det(\boldsymbol{Z})} \int_{|\boldsymbol{\zeta}|=1} \check{\mathbf{H}}(\boldsymbol{\zeta})|\boldsymbol{Z}^{-1}\cdot\boldsymbol{\zeta}|^{-3}\,dS, \tag{53}$$

with $\check{H}_{ijkl} = (L_{iakb}\zeta_a\zeta_b)^{-1}\zeta_j\zeta_l|_{[ij](kl)}$ (the square brackets denote the skew-symmetric part of the first two indices, whereas the simple brackets define the symmetric part of the last two indices). The second-order tensor $\boldsymbol{Z}$ serves to characterize the *instantaneous* shape and orientation of the voids and their distribution function and is given by relation (22). Note that the limit of incompressibility (i.e., $\kappa \to \infty$) needs to be considered for the evaluation of the term $\boldsymbol{\Pi}\mathbf{L}$ in (53) (the expressions are too cumbersome to be included here).

4. Evolution of microstructure

When viscoplastic porous materials undergo finite deformations, their microstructure and thus the anisotropy of the material evolve. The evolution laws of the microstructural variables complete the constitutive model. As discussed in prior work (Ponte Castañeda and Zaidman, 1994; Kailasam and Ponte Castañeda, 1998; Aravas and Ponte Castañeda, 2004), the purpose of homogenization theories is the description of the effective behavior of the composite in *average* terms. For this reason, it makes sense to consider that the initially ellipsoidal voids will evolve—on average—to ellipsoidal voids with different shape and orientation. This consideration suggests that the evolution of the shape and orientation of the pores may be approximated by the average strain-rate $\bar{\boldsymbol{D}}^{(2)}$ and spin $\bar{\boldsymbol{\Omega}}^{(2)}$ in the vacuous phase, which can be easily obtained as a byproduct of the homogenization methods described in the previous section. We can derive evolution laws for the microstructural variables simply by making use of the kinematics of the problem. These laws are presented below.

Porosity. The incompressibility of the matrix phase, implies that the evolution law for the porosity is given by

$$\dot{f} = (1-f)\bar{D}_{ii}, \tag{54}$$

with $\bar{\boldsymbol{D}}$ given by relation (31).

Aspect ratios. The evolution of the aspect ratios of the ellipsoidal void is defined by

$$\dot{w}_i = w_i\big(\mathbf{n}^{(3)}\cdot\bar{\boldsymbol{D}}^{(2)}\mathbf{n}^{(3)} - \mathbf{n}^{(i)}\cdot\bar{\boldsymbol{D}}^{(2)}\mathbf{n}^{(i)}\big)$$
$$= w_i\big(\mathbf{n}^{(3)}\otimes\mathbf{n}^{(3)} - \mathbf{n}^{(i)}\otimes\mathbf{n}^{(i)}\big)\cdot\bar{\boldsymbol{D}}^{(2)}, \tag{55}$$

(no sum on $i = 1, 2$), where the average strain-rate in the void $\bar{\boldsymbol{D}}^{(2)}$ is computed by relation (52). It should be emphasized at this point that, unlike expression (54), which is exact, relation (55) is only approximate in the sense of the assumption (already discussed) that the voids evolve—on average—to ellipsoidal voids (with different size, shape and orientation).

Orientation vectors. The evolution of the orientation vectors $\mathbf{n}^{(i)}$ is determined by the spin of the Eulerian axes of the ellipsoidal voids, or "microstructural" spin $\boldsymbol{\omega}$, via

$$\dot{\mathbf{n}}^{(i)} = \boldsymbol{\omega}\mathbf{n}^{(i)}, \quad i = 1, 2, 3. \tag{56}$$

The microstructural spin $\boldsymbol{\omega}$ is related to the average spin in the void, $\bar{\boldsymbol{\Omega}}^{(2)}$, and the average strain-rate in the void, $\bar{\boldsymbol{D}}^{(2)}$, by the well-known kinematical relation, which is written in direct notation as (Hill, 1978; Aravas and Ponte Castañeda, 2004)

$$\boldsymbol{\omega} = \bar{\boldsymbol{\Omega}}^{(2)} + \frac{1}{2}\sum_{\substack{i,j=1\\ i\neq j\\ w_i\neq w_j}}^{3} \frac{w_i^2 + w_j^2}{w_i^2 - w_j^2}\big[\big(\mathbf{n}^{(i)}\otimes\mathbf{n}^{(j)} + \mathbf{n}^{(j)}\otimes\mathbf{n}^{(i)}\big)\cdot\bar{\boldsymbol{D}}^{(2)}\big]$$
$$\times\,\mathbf{n}^{(i)}\otimes\mathbf{n}^{(j)}, \tag{57}$$

with $w_3 = 1$. The special case in which at least two aspect ratios are equal is discussed in detail later in this section.

For later use, it is pertinent to discuss, here, the evaluation of the Jaumann rate of the orientation vectors $\mathbf{n}^{(i)}$, denoted by $\overset{\triangledown}{\mathbf{n}}{}^{(i)}$ ($i = 1, 2, 3$), which is related to the standard time derivative of relation (56) by

$$\overset{\triangledown}{\mathbf{n}}{}^{(i)} = \dot{\mathbf{n}}^{(i)} - \bar{\boldsymbol{\Omega}}\mathbf{n}^{(i)} = (\boldsymbol{\omega} - \bar{\boldsymbol{\Omega}})\mathbf{n}^{(i)}, \quad i = 1, 2, 3. \tag{58}$$

The last equation can be written in terms of the *plastic* spin (Dafalias, 1985), which is defined as the spin of the continuum relative to the microstructure, as follows

$$\overset{\triangledown}{\mathbf{n}}{}^{(i)} = -\boldsymbol{\Omega}^p\mathbf{n}^{(i)} \quad \text{with } \boldsymbol{\Omega}^p = \bar{\boldsymbol{\Omega}} - \boldsymbol{\omega}. \tag{59}$$

At this point, it should be remarked that special care needs to be taken for the computation of the spin of the Eulerian axes in the case of a spherical void, i.e., when $w_1 = w_2 = w_3 = 1$, as well as for a spheroidal void, i.e., when $w_1 = w_2 \neq w_3 = 1$ or $w_1 \neq w_2 = w_3 = 1$ or $w_1 = w_3 = 1 \neq w_2$. More specifically, when two of the aspect ratios are equal, for instance $w_1 = w_2$, the material becomes transversely isotropic about the $\mathbf{n}^{(3)}$—direction, and thus the component Ω_{12}^p becomes indeterminate. Since the spin Ω_{12}^p is inconsequential in this case, it can be set equal to zero (Aravas, 1992), which implies that $\omega_{12} = \bar{\Omega}_{12}$. This notion can be applied whenever the shape of the void is spheroidal, in any given orientation. Following a similar line of thought, when the voids are spherical ($w_1 = w_2 = w_3 = 1$) the material is isotropic so that $\boldsymbol{\Omega}^p = \mathbf{0}$, $\overset{\triangledown}{\mathbf{n}}{}^{(i)} = 0$ and $\dot{\mathbf{n}}^{(i)} = \bar{\boldsymbol{\Omega}}\mathbf{n}^{(i)}$.

5. Porous materials with an ideally-plastic matrix phase

In this section, we specialize the results reported in the previous sections to the special, albeit important, case of porous materials with an ideally-plastic matrix phase. For this, we need to consider the ideally-plastic limit as $n \to \infty$ (or, equivalently, $m \to 0$) for the nonlinear exponent of the matrix phase.

In this regard, it is useful to study this limit in connection with the general definition of the gauge function in (10). Making use of definition (7) in the ideally-plastic limit, the effective stress potential $\tilde{U}$ of the porous medium becomes (Suquet, 1983, 1993)

$$\tilde{U}(\bar{\boldsymbol{\sigma}}; s_\alpha) = \begin{cases} 0, & \text{if } \Gamma_\infty(\bar{\boldsymbol{\sigma}}; s_\alpha)/\sigma_o \leqslant 1, \\ \infty, & \text{otherwise.} \end{cases} \tag{60}$$

This implies that the equation describing the yield locus is $\Gamma_\infty(\bar{\boldsymbol{\sigma}}) = \sigma_o$, which together with (9) shows that $\bar{\boldsymbol{\Sigma}} = \bar{\boldsymbol{\sigma}}/\sigma_o$ in the limit as $n \to \infty$. Then, in the ideally-plastic limit, it follows from (10) that the gauge function can be expressed as

$$\tilde{\Phi}_\infty(\bar{\boldsymbol{\Sigma}}; s_\alpha) = \Gamma_\infty(\bar{\boldsymbol{\Sigma}}; s_\alpha) - 1 = \Gamma_\infty(\bar{\boldsymbol{\sigma}}/\sigma_o; s_\alpha) - 1 = \tilde{\Phi}_\infty(\bar{\boldsymbol{\sigma}}/\sigma_o; s_\alpha), \tag{61}$$

so that $\tilde{\Phi}_\infty(\bar{\boldsymbol{\Sigma}}) = 0$ defines the corresponding gauge surface

$$\mathcal{P}_\infty \equiv \{\bar{\boldsymbol{\Sigma}}, \Gamma_\infty(\bar{\boldsymbol{\Sigma}}; s_\alpha) = 1\}. \tag{62}$$

It is convenient to define the yield criterion in terms of the macroscopic stress $\bar{\boldsymbol{\sigma}}$. This can be easily extracted from (61) by making use of the fact that Γ_n is a positively homogeneous function of degree one in $\bar{\boldsymbol{\sigma}}/\sigma_o$, so that

$$\tilde{\Phi}(\bar{\boldsymbol{\sigma}}; s_\alpha) = \sigma_o \tilde{\Phi}_\infty(\bar{\boldsymbol{\sigma}}; s_\alpha) = \sigma_o \Gamma_\infty(\bar{\boldsymbol{\sigma}}/\sigma_o; s_\alpha) - \sigma_o = \Gamma_\infty(\bar{\boldsymbol{\sigma}}; s_\alpha) - \sigma_o. \tag{63}$$

Then, the yield criterion $\tilde{\Phi}(\bar{\boldsymbol{\sigma}}) = 0$ describes the yield surface

$$\mathcal{P} \equiv \{\bar{\boldsymbol{\sigma}}, \Gamma_\infty(\bar{\boldsymbol{\sigma}}; s_\alpha) = \sigma_o\}, \tag{64}$$

which is a homothetic expansion by a factor of σ_o of the gauge surface $\mathcal{P}_\infty$ defined by (62).

5.1. "Second-order" estimates

In the context of the *SOM* method, the definition of the effective yield function requires special attention in that we first have to identify the terms in (29) that remain in the ideally-plastic limit. In this connection, it can be verified from definition (25) and (28) that

$$\hat{\sigma}_{\text{eq}} > \hat{\sigma}_{\|} \geqslant \check{\sigma}_{\text{eq}} \geqslant 0. \tag{65}$$

Consequently, as $n \to \infty$ the second term of relation (29), $(\frac{\check{\sigma}_{\text{eq}}}{\sigma_o})^n$, goes faster to zero than the first term $(\hat{\sigma}_{\text{eq}}/\sigma_o)^{n+1}$, provided that $\hat{\sigma}_{\text{eq}} < \sigma_o$.

Then, by considering the limit $n \to \infty$ in (30) and taking into account the inequalities (65), the yield function (63) associated with the *SOM* can be expressed by

$$\tilde{\Phi}(\bar{\boldsymbol{\sigma}}; s_\alpha) = \Gamma_\infty^{\text{som}}(\bar{\boldsymbol{\sigma}}; s_\alpha) - \sigma_o = \hat{\sigma}_{\text{eq}}(\bar{\boldsymbol{\sigma}}; \check{\boldsymbol{\sigma}}, k, s_\alpha) - \sigma_o, \tag{66}$$

where s_α is the set of the microstructural variables defined by (2), k is the anisotropy ratio in the LCC defined by (17), and $\check{\boldsymbol{\sigma}}$ is the reference stress tensor given by (39), (40). The evaluation of $\check{\boldsymbol{\sigma}}$ in the ideally-plastic limit is similar to that described in Subsection 3.3 and is detailed in Appendix C. On the other hand, k is determined by the solution of (27), which reduces to

$$(k-1)\frac{\hat{\sigma}_{\|}}{\check{\sigma}_{\text{eq}}} + 1 = 0, \tag{67}$$

in the limit as $n \to \infty$. (Recall that $\hat{\sigma}_{\|}$ is a function of k given by (28).)

The corresponding macroscopic strain-rate is obtained by differentiating the effective yield function with respect to $\bar{\boldsymbol{\sigma}}$ (i.e., associative flow rule), so that

$$\bar{\boldsymbol{D}} = \dot{\Lambda}\frac{\partial \tilde{\Phi}}{\partial \bar{\boldsymbol{\sigma}}} = \dot{\Lambda}\frac{\partial \hat{\sigma}_{\text{eq}}}{\partial \bar{\boldsymbol{\sigma}}}. \tag{68}$$

Here, $\dot{\Lambda}$ is a nonnegative plastic multiplier to be determined from the consistency condition $\dot{\tilde{\Phi}} = 0$, which reads (by noting that $\tilde{\Phi}$ is an isotropic function of its arguments (Dafalias, 1985))

$$\dot{\tilde{\Phi}} = \frac{\partial \tilde{\Phi}}{\partial \bar{\boldsymbol{\sigma}}} \cdot \overset{\triangledown}{\bar{\boldsymbol{\sigma}}} + \frac{\partial \tilde{\Phi}}{\partial s_\alpha} \overset{\triangledown}{s}_\alpha = 0, \tag{69}$$

with the symbol $\overset{\triangledown}{()}$ denoting the Jaumann rate of a given quantity.[1]

[1] The Jaumann rates associated with a second-order tensor $\boldsymbol{A}$, a vector $\mathbf{a}$, and a scalar f, are such that $\overset{\triangledown}{\boldsymbol{A}} = \dot{\boldsymbol{A}} + \boldsymbol{A}\bar{\boldsymbol{\Omega}} - \bar{\boldsymbol{\Omega}}\boldsymbol{A}$, $\overset{\triangledown}{\mathbf{a}} = \dot{\mathbf{a}} - \bar{\boldsymbol{\Omega}}\mathbf{a}$, and $\overset{\triangledown}{f} = \dot{f}$. Here, $\bar{\boldsymbol{\Omega}}$ denotes the macroscopic spin tensor.

The term $\overset{\triangledown}{s}_\alpha$ will be shown in the sequel to be proportional to the plastic multiplier $\dot{\Lambda}$. This proportionality (considered as given here) allows us to define a scalar function, known as the Jaumann hardening rate H_J, which is independent of $\dot{\Lambda}$, via

$$\dot{\Lambda} H_J = -\frac{\partial \tilde{\Phi}}{\partial s_\alpha}\overset{\triangledown}{s}_\alpha. \tag{70}$$

The Jaumann hardening rate H_J is an objective measure of the geometrical softening or hardening of the porous material to be used in the prediction of macroscopic instabilities in Part II of this work. Use of (70) in relation (69) gives

$$\dot{\tilde{\Phi}} = \frac{\partial \tilde{\Phi}}{\partial \bar{\boldsymbol{\sigma}}} \cdot \overset{\triangledown}{\bar{\boldsymbol{\sigma}}} - \dot{\Lambda} H_J = 0 \quad \Rightarrow \quad \dot{\Lambda} = \frac{1}{H_J}\frac{\partial \tilde{\Phi}}{\partial \bar{\boldsymbol{\sigma}}} \cdot \overset{\triangledown}{\bar{\boldsymbol{\sigma}}}. \tag{71}$$

Then, substituting (71) in (68), one finds that

$$\bar{D}_{ij} = \frac{1}{H_J}\frac{\partial \tilde{\Phi}}{\partial \bar{\sigma}_{ij}}\frac{\partial \tilde{\Phi}}{\partial \bar{\sigma}_{kl}}\overset{\triangledown}{\bar{\sigma}}_{kl}. \tag{72}$$

It should be emphasized here that although the behavior of the matrix is ideally-plastic, the corresponding effective behavior of the porous medium can exhibit hardening ($H_J > 0$) or softening ($H_J < 0$) due to the evolution of the underlying microstructure when subjected to finite deformations.

It is important to note that strain hardening and temperature effects can be accounted for in a straightforward manner by allowing the yield stress σ_o in (66) depend on the equivalent plastic strain $\bar{\varepsilon}_p^{(1)}$ in the matrix phase (Aravas, 1987; Aravas and Ponte Castañeda, 2004) and temperature T (Klöcker and Tvergaard, 2003), such that $\sigma_o = \sigma_o(\bar{\varepsilon}_p^{(1)}, T)$. However, the main goal in this study is to examine the effect of the evolution of microstructure on the overall behavior of the porous material and for this reason we will assume that σ_o remains constant during the deformation process, thus neglecting any temperature and strain hardening effects.

5.2. Relation between the plastic multiplier and the shear modulus

To establish relation (71), we have considered (as given) that $\overset{\triangledown}{s}_\alpha$ is proportional to the plastic multiplier $\dot{\Lambda}$. To demonstrate this proportionality condition, we will first show that $1/\mu$ is proportional to the plastic multiplier $\dot{\Lambda}$. For this purpose, we consider the derivative with respect to $\bar{\boldsymbol{\sigma}}$ in expression (29), which together with the secant condition $(26)_2$ and the inequalities (65), leads to the following result:

$$\bar{\boldsymbol{D}} = \frac{(1-f)\sigma_o}{3\mu}\left(\frac{\hat{\sigma}_{\text{eq}}}{\sigma_o}\right)\frac{\partial \hat{\sigma}_{\text{eq}}}{\partial \bar{\boldsymbol{\sigma}}} \quad \text{as } n \to \infty. \tag{73}$$

Comparing (68) with (73), one deduces that

$$\dot{\Lambda} = \frac{(1-f)\sigma_o}{3\mu}\left(\frac{\hat{\sigma}_{\text{eq}}}{\sigma_o}\right). \tag{74}$$

Obviously, when the yield condition (66) is not satisfied, i.e., $\hat{\sigma}_{\text{eq}} < \sigma_o$, $\mu \to \infty$ (from $(26)_2$) or equivalently $\dot{\Lambda} = 0$. On the other hand, when $\hat{\sigma}_{\text{eq}} = \sigma_o$, relation (74) becomes

$$\frac{1}{\mu} = \frac{3\dot{\Lambda}}{(1-f)\sigma_o}. \tag{75}$$

It follows from this relation that the inverse of the shear modulus μ in the LCC is directly proportional to the plastic multiplier $\dot{\Lambda}$ in the ideally-plastic limit. Note that the above analysis is also valid in the context of the *VAR* method of Ponte Castañeda (1991) (see Danas (2008)). In the next subsection, we make use of (75) to show that $\overset{\triangledown}{s}_\alpha$ is proportional to the plastic multiplier $\dot{\Lambda}$.

5.3. Computation of the Jaumann hardening rate

In order to derive an expression for H_J, it is essential to write the evolution laws for the microstructural variables, presented in Section 4, in such a way that they are proportional to the plastic multiplier $\dot{\Lambda}$, or equivalently to $1/\mu$. From this viewpoint, it is easily shown that in the incompressibility limit $\kappa \to \infty$, the fourth-order tensor $\mathbf{M}$ (see (14)) is proportional to $1/\mu$ and consequently to $\dot{\Lambda}$, i.e., $\mathbf{M} = \boldsymbol{\mathcal{M}}(k)/\mu$, where $\boldsymbol{\mathcal{M}}$ is independent of μ. Similarly, it can be verified that the microstructural tensor $\mathbf{Q}$ is also proportional to $1/\mu$, such that $\mathbf{Q} = \mu\widehat{\mathbf{Q}}(k)$, whereas the tensor $\mathbf{\Pi L}$ is independent of μ (the relevant expressions are too cumbersome to be included here).

In connection with these last results, it follows from (52) and (75) that

$$\bar{\boldsymbol{D}}^{(2)} = \dot{\Lambda}\left\{\frac{1}{3f}\frac{\partial\tilde{\Phi}}{\partial\bar{\sigma}_{ii}} + \frac{3}{1-f}\mathbf{K}\left(\frac{3}{1-f}\widehat{\mathbf{Q}}(k)^{-1}\frac{\bar{\boldsymbol{\sigma}}}{\sigma_o} - \boldsymbol{\mathcal{M}}(k)\frac{\check{\boldsymbol{\sigma}}}{\sigma_o}\right)\right\}, \quad (76)$$

where use was made of the fact that in the ideally-plastic limit $\boldsymbol{\eta} = -\mathbf{M}\check{\boldsymbol{\sigma}}$ (see relation (19) and (65) noting that $\check{\sigma}_{eq} < \sigma_o$ as $n \to \infty$). In turn, making use of (53) and (75), we can express the relative average spin tensor $\bar{\boldsymbol{\Omega}}^{(2)} - \bar{\boldsymbol{\Omega}}$ as

$$\bar{\boldsymbol{\Omega}}^{(2)} - \bar{\boldsymbol{\Omega}} = \mathbf{\Pi L}\mathbf{Q}^{-1}\bar{\boldsymbol{\sigma}} = \dot{\Lambda}\frac{3}{1-f}\mathbf{\Pi L}\widehat{\mathbf{Q}}(k)^{-1}\frac{\bar{\boldsymbol{\sigma}}}{\sigma_o}. \quad (77)$$

Relations (76) and (77) allow us to write the evolution laws of Section 4 in terms of $\dot{\Lambda}$, such that

$$\dot{f} = (1-f)\bar{D}_{ii} = \dot{\Lambda}y_f(\bar{\boldsymbol{\sigma}};\check{\boldsymbol{\sigma}},k,s_\alpha)$$
$$\text{with } y_f(\bar{\boldsymbol{\sigma}};\check{\boldsymbol{\sigma}},k,s_\alpha) = (1-f)\frac{\partial\tilde{\Phi}}{\partial\bar{\sigma}_{ii}}, \quad (78)$$

and

$$\dot{w}_i = w_i\left(\mathbf{n}^{(3)}\otimes\mathbf{n}^{(3)} - \mathbf{n}^{(i)}\otimes\mathbf{n}^{(i)}\right)\cdot\bar{\boldsymbol{D}}^{(2)} = \dot{\Lambda}y_w^{(i)}(\bar{\boldsymbol{\sigma}};\check{\boldsymbol{\sigma}},k,s_\alpha) \quad (79)$$

with

$$y_w^{(i)}(\bar{\boldsymbol{\sigma}};\check{\boldsymbol{\sigma}},k,s_\alpha) = w_i\left(\mathbf{n}^{(3)}\otimes\mathbf{n}^{(3)} - \mathbf{n}^{(i)}\otimes\mathbf{n}^{(i)}\right) \times\frac{3}{1-f}\mathbf{K}\left(\frac{3}{1-f}\widehat{\mathbf{Q}}(k)^{-1}\frac{\bar{\boldsymbol{\sigma}}}{\sigma_o} - \boldsymbol{\mathcal{M}}(k)\frac{\check{\boldsymbol{\sigma}}}{\sigma_o}\right), \quad (80)$$

(no sum on $i = 1, 2$). In these expressions, y_f and $y_w^{(i)}$ are smooth functions of their arguments. In turn, it follows from (57), (58), $(59)_2$ and (76) that

$$\boldsymbol{\Omega}^p = \bar{\boldsymbol{\Omega}} - \boldsymbol{\omega} = -\dot{\Lambda}\boldsymbol{y}_n^{(i)}(\bar{\boldsymbol{\sigma}};\check{\boldsymbol{\sigma}},k,s_\alpha)$$
$$\Rightarrow \overset{\triangledown}{\mathbf{n}}{}^{(i)} = \dot{\Lambda}\boldsymbol{y}_n^{(i)}(\bar{\boldsymbol{\sigma}};\check{\boldsymbol{\sigma}},k,s_\alpha)\mathbf{n}^{(i)}. \quad (81)$$

In this expression, $\boldsymbol{y}_n^{(i)}$ are skew-symmetric, second-order tensors defined as

$$\boldsymbol{y}_n^{(i)}(\bar{\boldsymbol{\sigma}};\check{\boldsymbol{\sigma}},k,s_\alpha) = \frac{3}{1-f}\mathbf{\Pi L}\widehat{\mathbf{Q}}(k)^{-1}\frac{\bar{\boldsymbol{\sigma}}}{\sigma_o} + \frac{1}{2}\sum_{\substack{i,j=1\\ i\neq j\\ w_i\neq w_j}}^{3}\mathcal{X}_{(ij)}\mathbf{n}^{(i)}\otimes\mathbf{n}^{(j)}, \quad (82)$$

with

$$\mathcal{X}_{(ij)} = \frac{w_i^2 + w_j^2}{w_i^2 - w_j^2}\left[\left(\mathbf{n}^{(i)}\otimes\mathbf{n}^{(j)} + \mathbf{n}^{(j)}\otimes\mathbf{n}^{(i)}\right) \times\frac{3}{1-f}\mathbf{K}\left(\frac{3}{1-f}\widehat{\mathbf{Q}}(k)^{-1}\frac{\bar{\boldsymbol{\sigma}}}{\sigma_o} - \boldsymbol{\mathcal{M}}(k)\frac{\check{\boldsymbol{\sigma}}}{\sigma_o}\right)\right]. \quad (83)$$

Finally, it follows from (70), that the Jaumann hardening rate is given by

$$H_J = -\frac{1}{\dot{\Lambda}}\frac{\partial\tilde{\Phi}}{\partial s_\alpha}\overset{\triangledown}{s}_\alpha = -\left\{y_f\frac{\partial\tilde{\Phi}}{\partial f} + \sum_{i=1}^{2}y_w^{(i)}\frac{\partial\tilde{\Phi}}{\partial w_i} + \sum_{i=1}^{3}\frac{\partial\tilde{\Phi}}{\partial\mathbf{n}^{(i)}}\cdot\boldsymbol{y}_n^{(i)}\mathbf{n}^{(i)}\right\}. \quad (84)$$

6. Concluding remarks

In this work, a constitutive model has been developed for porous media with viscoplastic (including ideally-plastic) matrix phases and particulate microstructures subjected to general three-dimensional finite deformations. The theoretical framework of the model is based on the rigorous nonlinear "second-order" homogenization method of Ponte Castañeda (2002a), which is valid for general "ellipsoidal" microstructures and loading conditions. In particular, the present study comprised two main parts: (1) the determination of the instantaneous effective behavior of a porous medium with aligned ellipsoidal voids distributed randomly in the representative volume element for general loading conditions and (2) the characterization of the microstructure via appropriate evolution laws for the internal variables defining the state of the microstructure at a given instant.

The main improvement of the present model over the earlier "variational" model of Ponte Castañeda (1991) (Ponte Castañeda and Zaidman, 1994; Kailasam and Ponte Castañeda, 1998; Aravas and Ponte Castañeda, 2004) is a result of the fact that the new model is able to reproduce exactly the behavior of a "composite-sphere assemblage" in the limit of hydrostatic loadings, and therefore coincides with the hydrostatic limit of Gurson's criterion in the special case of ideal plasticity and isotropic microstructures. In addition, the model has been extended to general ellipsoidal microstructures and loading conditions by appropriate scaling of the "variational" estimates, which are known to be too stiff at purely hydrostatic loadings.

By contrast with other models proposed in the literature (Gologanu et al., 1997; Gărăjeu et al., 2000; Flandi and Leblond, 2005a; Monchiet et al., 2007) that are valid only for spheroidal voids (i.e., transversely isotropic symmetry of the material) and axisymmetric loading conditions aligned with the pore symmetry axis, the present model is capable of handling more general "ellipsoidal" microstructures (i.e., orthotropic symmetry of the material) and arbitrary three-dimensional loading conditions. This, in turn, allows for the implementation of the present model in a general purpose subroutine—similar to the earlier works of Kailasam et al. (2000) and Aravas and Ponte Castañeda (2004) in the context of the "variational" method—appropriate for large-scale finite element calculations to study complex problems of practical and theoretical interest (i.e., forming processes, structural integrity assessment, ductile fracture of voided metals, plastic flow localization and necking in plane-strain or plane-stress tension, structural behavior of porous metals with directional pores, etc.).

Finally, it should be mentioned that several important issues, such as elasticity, strain-hardening and thermal effects, that were neglected for simplicity in this first paper will be considered in future work. We are confident that the present model can be readily extended to deal with the aforementioned issues in a straightforward manner while still being able to account for anisotropic microstructures and general loading conditions. Thus, the new model is expected to be complementary to the recent studies of Gologanu et al. (2001a, 2001b), Pardoen and Hutchinson (2000) and Benzerga (2002) for coalescence and Nahshon and Hutchinson (2008), Leblond and Mottet (2008) and Xue (2008) for shear failure, which are strictly valid only for loading conditions that are consistent with the development of isotropic or transversely isotropic symmetries.

Acknowledgements

The authors would like to thank Professor Nikolaos Aravas for his valuable comments on this manuscript. The work of K.D. was supported by the international fellowship "Gaspard Monge" at the École Polytechnique and partially by the scholarship for Hellenes of the Alexander S. Onassis Public Benefit Foundation. The work of K.D. and P.P.C. was also supported by the US National Science Foundation through Grants CMS-02-01454 and OISE-02-31867. A FORTRAN subroutine for the numerical integration of the above-discussed model is available upon request.

Appendix A. The coefficients of the reference stress tensor

The coefficients introduced in relation (40) are given by

$$\beta_1(X_\Sigma, f) = \frac{1+X_\Sigma^4}{1+2\beta_3(f)X_\Sigma^2+X_\Sigma^4},$$
$$\text{with } \beta_3(f) = 10\left(1-\left(\frac{\arctan(10^4 f^3/\exp(-f))}{\pi/2}\right)^4\right), \tag{85}$$

and

$$\beta_2(f,n) = \frac{2}{e}\frac{38}{n^2+10}\left(1-\left(\frac{\arctan(10^4 f^2/\exp(-500f))}{\pi/2}\right)^6\right). \tag{86}$$

It should be emphasized that the coefficient β_2 becomes approximately zero for porosities larger than 1% and for very high nonlinearities (i.e., $n > 10$) and hence the terms containing β_2 in the definition of the reference stress tensor in relation (40) could be neglected in these cases. In particular, $\beta_2 = 0$ in the ideally-plastic limit $n \to \infty$.

Appendix B. Evaluation of the hydrostatic point

In this section, we discuss briefly the determination of the mean normalized stress $\bar{\Sigma}_m^H$, which is necessary for the evaluation of the factor α_{eq} in the context of relation (44).

Combining relations (7) and (33), we can easily express the gauge factor Γ_n as a function of the macroscopic mean stress $\bar{\sigma}_m$ via

$$\Gamma_n(\bar{\boldsymbol{\sigma}}) = \frac{3}{2}\left(\frac{\sigma_o}{\tilde{\sigma}_w}\right)^{\frac{n}{n+1}}|\bar{\sigma}_m| \quad \Rightarrow \quad |\bar{\Sigma}_m| = \frac{2}{3}\left(\frac{\tilde{\sigma}_w}{\sigma_o}\right)^{\frac{n}{n+1}} \equiv \bar{\Sigma}_m^H. \tag{87}$$

Here, use of the definition of the normalized stress $\bar{\boldsymbol{\Sigma}}$ in (9) was made. Subsequently, it follows from (87) that

$$\bar{\Sigma}_m^H\big|_{\text{som}} = \frac{2}{3}\left(\frac{\tilde{\sigma}_w}{\sigma_o}\right)^{\frac{n}{n+1}} \quad \text{and} \quad \bar{\Sigma}_m^H\big|_{\text{var}} = \frac{2}{3}\left(\frac{\tilde{\sigma}_w^{\text{var}}}{\sigma_o}\right)^{\frac{n}{n+1}} \tag{88}$$

with $\tilde{\sigma}_w$ and $\tilde{\sigma}_w^{\text{var}}$ given by (37) and (38), respectively. Note that in the special case of ideal-plasticity ($n \to \infty$), (87) reduces to

$$|\bar{\Sigma}_m| = \frac{2}{3}\frac{\tilde{\sigma}_w}{\sigma_o} \equiv \bar{\Sigma}_m^H. \tag{89}$$

Appendix C. Reference stress tensor for an ideally-plastic matrix phase

In this section, we discuss briefly the computation of the reference stress $\check{\sigma}_{\text{eq}}$ in the ideally-plastic limit ($n \to \infty$).

In connection with the procedure detailed in Subsection 3.3, for the computation of $\check{\boldsymbol{\sigma}}$, we need to compute the two coefficients α_m and α_{eq}, defined in the context of relations (39) and (40). The evaluation of these two scalars has been provided schematically in (41) and (42). In order to compute α_m, first, we need to provide the expressions for the determination of the effective flow stresses $\tilde{\sigma}_{w=1}$ and $\tilde{\sigma}_{w=1}^{\text{var}}$ associated with the spherical shell problem and the corresponding *VAR* estimate for spherical voids, respectively, in the ideally-plastic limit. Consideration of the limit $n \to \infty$ in (34) and (35) leads to the well known results

$$\frac{\tilde{\sigma}_{w=1}}{\sigma_o} = \ln\left(\frac{1}{f}\right) \quad \text{and} \quad \frac{\tilde{\sigma}_{w=1}^{\text{var}}}{\sigma_o} = \frac{1-f}{\sqrt{f}}. \tag{90}$$

According to relation (36), the effective flow stress for any combination of aspect ratios w_1 and w_2 is approximated by

$$\tilde{\sigma}_w = \frac{\tilde{\sigma}_{w=1}}{\tilde{\sigma}_{w=1}^{\text{var}}}\tilde{\sigma}_w^{\text{var}}, \qquad \tilde{\sigma}_w^{\text{var}} = \left[\frac{4\boldsymbol{\delta}\cdot\widehat{\mathbf{M}}\boldsymbol{\delta}}{3(1-f)\sigma_o^2}\right]^{-\frac{1}{2}}. \tag{91}$$

Here, $\tilde{\sigma}_w^{\text{var}}$ is derived by taking the limit $n \to \infty$ in (38) and corresponds to the effective hydrostatic flow stress delivered by the *VAR* procedure in the context of ideally-plastic porous media, whereas $\widehat{\mathbf{M}}$ is given by $(38)_2$. This result in combination with relations (39) and (41) allows the computation of the coefficient α_m from the relation

$$\tilde{\Phi}(\bar{\sigma}_m; \check{\boldsymbol{\sigma}}, f, w_1, w_2) = \hat{\sigma}_{\text{eq}}(\bar{\sigma}_m; \check{\boldsymbol{\sigma}}, k^H, f, w_1, w_2) - \sigma_o = 0, \tag{92}$$

with $\bar{\sigma}_m = 2\tilde{\sigma}_w/3$. Note that the anisotropy ratio k^H is determined by the nonlinear equation (67), in the hydrostatic limit, while the effective yield function $\tilde{\Phi}$ has been defined in (66).

The coefficient α_{eq} can be computed by taking the limit $n \to \infty$ in relation (44), so that

$$\alpha_{\text{eq}} = \alpha_m^{-1}\left[1 + \frac{2k^H(\bar{d}_\parallel - \bar{d}_{\text{var}}) - \check{\sigma}_{\text{eq}}}{(1-f)\hat{\sigma}_\parallel}\right]. \tag{93}$$

All the quantities involved in (93) are evaluated in the hydrostatic limit $X_\Sigma \to \pm\infty$. In particular, $\bar{d}_\parallel = \text{sgn}(X_\Sigma)\tilde{\sigma}_w\bar{\mathbf{S}}\cdot\tilde{\mathbf{M}}(k^H, \mu = 1)\boldsymbol{\delta}$, and $\bar{d}_{\text{var}} = \text{sgn}(X_\Sigma)\tilde{\sigma}_w^{\text{var}}\bar{\mathbf{S}}\cdot\widehat{\mathbf{M}}\boldsymbol{\delta}$.

In the context of these results for the special case of porous materials with an ideally-plastic matrix phase, expressions (42) (or (93)) are assumed to hold for all stress states, which implies that the resulting effective yield surface remains smooth for the entire range of the stress triaxialities. Further support for this last assumption arises from the fact that—to the best knowledge of the authors—there is no definitive numerical or experimental evidence implying the existence of a vertex in the hydrostatic limit for general isotropic or ellipsoidal microstructures, in contrast with transversely isotropic microstructures, where the existence of a corner may be observed in yield surfaces obtained by limit analysis procedures (Pastor and Ponte Castañeda, 2002).

Appendix D. Numerical implementation

In this section, we describe the numerical integration of the constitutive equations developed in the context of porous media with viscoplastic or ideally-plastic matrix phase. First, it is essential to define the boundary conditions in the problem. For convenience, we will consider here that velocity boundary conditions are given (see (3)) such that

$$\mathbf{v} = \bar{\mathbf{L}}\mathbf{x}, \quad \text{on } \partial\Omega, \tag{94}$$

where $\bar{\boldsymbol{L}}$ is the macroscopic velocity gradient. The symmetric and skew-symmetric part of $\bar{\boldsymbol{L}}$ denote the macroscopic strain-rate $\bar{\boldsymbol{D}}$ and spin $\bar{\boldsymbol{\Omega}}$, respectively. We define, then, the total displacement $\mathbf{u}$ in terms of the velocity $\mathbf{v}$ via

$$\mathbf{u} = \mathbf{v}t, \quad 0 < t < t_f, \tag{95}$$

where $\mathbf{v}$ is constant in time t and t_f is the total time.

In the following, the problem is solved incrementally using: (i) an implicit formulation for the estimation of the instantaneous response of the porous medium for a given microstructural configuration and (ii) an explicit scheme for the evolution of the microstructural variables s_α. First, we present the system of equations for the estimation of the instantaneous response of the porous medium making use of the methodology described in Section 3. Then, we update the values for the microstructural variables s_α as described in Section 4.

D.1. Estimation of the instantaneous response

Consider that the macroscopic (remote) average strain-rate $\bar{\boldsymbol{D}}$ and the values for the microstructural variables s_α are known in the beginning of the increment $t = t_j$, i.e.,

$$\bar{\boldsymbol{D}}, \qquad s_\alpha|_j, \tag{96}$$

where the subscript j is used to denote quantities at time t_j.

- ***Viscoplasticity***. At the end of the increment $t = t_{j+1}$, the following quantities need to be computed:

$$\bar{\boldsymbol{\sigma}}_{j+1}, \quad k_{j+1}, \quad \alpha_m|_{j+1}, \quad k^H_{j+1}, \tag{97}$$

where $\bar{\boldsymbol{\sigma}}$ is the macroscopic stress tensor, k is the anisotropy ratio of the matrix phase in the LCC, α_m is the factor involved in the computation of the reference stress tensor $\check{\boldsymbol{\sigma}}$ given by relation (41), and k^H is the anisotropy ratio of the matrix phase in the LCC in the purely hydrostatic limit ($|X_\Sigma| \to \infty$). For viscoplastic porous media, the above-mentioned unknowns are computed by the following from the following system of coupled, nonlinear, algebraic equations:

$$\begin{aligned}
&\bar{\boldsymbol{D}} = \frac{\partial \tilde{U}_{\text{som}}}{\partial \bar{\boldsymbol{\sigma}}}\big(\bar{\boldsymbol{\sigma}}_{j+1}; k_{j+1}, \alpha_m|_{j+1}, k^H_{j+1}, s_\alpha|_j\big),\\
&k_{j+1}\left(\frac{\hat{\sigma}_\parallel|_{j+1}}{\check{\sigma}_{\text{eq}}|_{j+1}}\right)^{1-n} = (k_{j+1}-1)\frac{\hat{\sigma}_\parallel|_{j+1}}{\check{\sigma}_{\text{eq}}|_{j+1}} + 1,\\
&\tilde{U}^H_{\text{som}}\big(\bar{\boldsymbol{\sigma}}' \to \mathbf{0}, \bar{\sigma}_m = 1; \alpha_m|_{j+1}, k^H_{j+1}, s_\alpha|_j\big)\\
&\quad = \frac{\dot{\varepsilon}_o \tilde{\sigma}_w}{1+n}\left(\frac{3}{2}\frac{|\bar{\sigma}_m|}{\tilde{\sigma}_w}\right)^{1+n}\bigg|_{\bar{\sigma}_m = 1},\\
&k^H_{j+1}\left(\frac{\hat{\sigma}_\parallel|^H_{j+1}}{\check{\sigma}_{\text{eq}}|^H_{j+1}}\right)^{1-n} = \big(k^H_{j+1}-1\big)\frac{\hat{\sigma}_\parallel|^H_{j+1}}{\check{\sigma}_{\text{eq}}|^H_{j+1}} + 1.
\end{aligned} \tag{98}$$

In these expressions, $\tilde{U}_{\text{som}}$ is given by (29), $\hat{\sigma}_{\text{eq}}$ and $\hat{\sigma}_\parallel$ are defined by (25) and (28), respectively, $\check{\sigma}_{\text{eq}}$ denotes the von Mises equivalent part of $\check{\boldsymbol{\sigma}}$ in (40) and $\tilde{\sigma}_w$ is evaluated by (34). As a consequence of the homogeneity of $\tilde{U}_{\text{som}}$ in $\bar{\boldsymbol{\sigma}}$, $\bar{\sigma}_m$ can be set equal to unity for simplicity. The superscript H has been used to emphasize that the quantities should be evaluated in the hydrostatic limit $|X_\Sigma| \to \infty$. It should be further emphasized that the way we consider the hydrostatic limit $|X_\Sigma| \to \infty$ or equivalently $\bar{\boldsymbol{\sigma}}' \to \mathbf{0}$ matters. This implies that the value of α_m will depend on the form of the normalized tensor $\bar{\boldsymbol{S}} = \bar{\boldsymbol{\sigma}}'/\bar{\sigma}_{\text{eq}}$ defined in (16). Note that the factor α_{eq}, needed for the evaluation of $\check{\boldsymbol{\sigma}}$ in (40), is computed by the analytical expression (44).

- ***Ideal plasticity***. At the end of the increment $t = t_{j+1}$, the following quantities need to be computed:

$$\bar{\boldsymbol{\sigma}}_{j+1}, \quad \dot{\Lambda}_{j+1}, \quad k_{j+1}, \quad \alpha_m|_{j+1}, \quad k^H_{j+1}, \tag{99}$$

where $\bar{\boldsymbol{\sigma}}$ is the macroscopic stress tensor, $\dot{\Lambda}$ denotes the plastic multiplier, k is the anisotropy ratio of the matrix phase in the LCC, α_m is the factor involved in the computation of the reference stress tensor $\check{\boldsymbol{\sigma}}$ given by relation (41), and k^H is the anisotropy ratio of the matrix phase in the LCC in the purely hydrostatic limit ($|X_\Sigma| \to \infty$). For porous media with an ideally-plastic matrix phase, the above-mentioned unknowns are computed from the following system of coupled, nonlinear, algebraic equations:

$$\begin{aligned}
&\bar{\boldsymbol{D}} = \dot{\Lambda}\frac{\partial \tilde{\Phi}}{\partial \bar{\boldsymbol{\sigma}}}\bigg|_{j+1},\\
&\tilde{\Phi}\big(\bar{\boldsymbol{\sigma}}_{j+1}; k_{j+1}, \alpha_m|_{j+1}, k^H_{j+1}, s_\alpha|_j\big) = 0,\\
&(k_{j+1}-1)\frac{\hat{\sigma}_\parallel|_{j+1}}{\check{\sigma}_{\text{eq}}|_{j+1}} + 1 = 0,\\
&\tilde{\Phi}\big(\bar{\boldsymbol{\sigma}}' \to \mathbf{0}, \bar{\sigma}_m = 2\tilde{\sigma}_w/3; \alpha_m|_{j+1}, k^H_{j+1}, s_\alpha|_j\big) = 0,\\
&\big(k^H_{j+1}-1\big)\frac{\hat{\sigma}_\parallel|^H_{j+1}}{\check{\sigma}_{\text{eq}}|^H_{j+1}} + 1 = 0,
\end{aligned} \tag{100}$$

where $\tilde{\Phi}$ is given by (66), $\hat{\sigma}_\parallel$ is defined by (28), $\check{\sigma}_{\text{eq}}$ denotes the von Mises equivalent part of $\check{\boldsymbol{\sigma}}$ in (40) and $\tilde{\sigma}_w$ is given by (91). Similar to the viscoplastic case, the superscript H has been used to denote the relevant quantities evaluated at the hydrostatic limit $|X_\Sigma| \to \infty$, while the factor α_{eq} (used in (40)) is computed by the analytical expression (93).

It is worth mentioning that in many cases of interest, the applied boundary conditions are such that the stress triaxiality X_Σ is constant during the deformation process. The above mentioned systems of equations can be easily modified to account for an imposed constraint on the stress triaxiality.

D.2. Update of the microstructural variables

Once, the macroscopic stress $\bar{\boldsymbol{\sigma}}$ (and the plastic multiplier $\dot{\Lambda}$ in ideal plasticity) is known, we can update the microstructural variables $s_\alpha|_{j+1}$ by using an explicit scheme with a time increment $\Delta t = t_{j+1} - t_j$, such that

$$f_{j+1} = f_j + (1 - f_j)\bar{D}_{ii}\Delta t, \tag{101}$$

$$w_1|_{j+1} = w_1|_j + \big(\mathbf{n}^{(3)}_j \cdot \bar{\boldsymbol{D}}^{(2)}\mathbf{n}^{(3)}_j - \mathbf{n}^{(1)}_j \cdot \bar{\boldsymbol{D}}^{(2)}\mathbf{n}^{(1)}_j\big)\Delta t, \tag{102}$$

$$w_2|_{j+1} = w_2|_j + \big(\mathbf{n}^{(3)}_j \cdot \bar{\boldsymbol{D}}^{(2)}\mathbf{n}^{(3)}_j - \mathbf{n}^{(2)}_j \cdot \bar{\boldsymbol{D}}^{(2)}\mathbf{n}^{(2)}_j\big)\Delta t, \tag{103}$$

$$\mathbf{n}^{(i)}_{j+1} = \mathbf{n}^{(i)}_j + \boldsymbol{\omega}\mathbf{n}^{(i)}_j\Delta t, \quad i = 1, 2, 3. \tag{104}$$

In these expressions, $\bar{\boldsymbol{D}}$ is prescribed or alternatively it could be evaluated by relation (31) for the viscoplastic case and (72) for the ideally-plastic case. The phase average tensors $\bar{\boldsymbol{D}}^{(2)}$ and $\boldsymbol{\omega}$ are computed by (52) and (57) for the viscoplastic case and by (76) and (81) for the ideally-plastic case.

Note further that in the last relation describing the evolution law for the orientation vectors $\mathbf{n}^{(i)}$, the usual explicit scheme leads to non-unit vectors due to the incremental approximation introduced in the problem. This can be resolved by integrating exactly the orientation vectors $\mathbf{n}^{(i)}$ (Aravas and Ponte Castañeda, 2004), which leads to

$$\mathbf{n}^{(i)}_{j+1} = \exp(\boldsymbol{\omega})\mathbf{n}^{(i)}_j, \quad i = 1, 2, 3. \tag{105}$$

The exponential of the skew-symmetric tensor $\boldsymbol{\omega}$ is an orthogonal tensor that can be determined from the following formula, attributed to Gibbs (Cheng and Gupta, 1989)

$$\exp(\boldsymbol{\omega}) = \boldsymbol{I} + \frac{\sin x}{x}\boldsymbol{\omega} + \frac{1-\cos x}{x^2}\boldsymbol{\omega}^2, \quad \text{with } x = \sqrt{\frac{1}{2}\boldsymbol{\omega}\cdot\boldsymbol{\omega}}. \tag{106}$$

The procedure discussed in this section is repeated until we reach the final prescribed time t_f defined by the user.

References

Aravas, N., 1987. On the numerical integration of a class of pressure-dependent plasticity models. Int. J. Numer. Meth. Engrg. 24, 1395–1416.

Aravas, N., 1992. Finite elastoplastic transformations of transversely isotropic metals. Int. J. Solids Struct. 29, 2137–2157.

Aravas, N., Ponte Castañeda, P., 2004. Numerical methods for porous metals with deformation-induced anisotropy. Comput. Methods Appl. Mech. Engrg. 193, 3767–3805.

Benzerga, A.A., 2002. Micromechanics of coalescence in ductile fracture. J. Mech. Phys. Solids 50, 1331–1362.

Bilger, N., Auslender, F., Bornert, M., Masson, R., 2002. New bounds and estimates for porous media with rigid perfectly plastic matrix. C. R. Mecanique 330, 127–132.

Bornert, M., Stolz, C., Zaoui, A., 1996. Morphologically representative pattern-based bounding in elasticity. J. Mech. Phys. Solids 44, 307–331.

Budiansky, B., Hutchinson, J.W., Slutsky, S., 1982. Void growth and collapse in viscous solids. In: Hopkins, H.G., Sewell, M.J. (Eds.), Mechanics of Solids, The Rodney Hill 60th anniversary Volume. Pergamon Press, Oxford, pp. 13–45.

Cheng, H., Gupta, K.C., 1989. A historical note on finite rotations. J. Appl. Mech. 56, 139–145.

Dafalias, Y.F., 1985. The plastic spin. J. Appl. Mech. 52, 865–871.

Danas, K., 2008. Homogenization-based constitutive models for viscoplastic porous media with evolving microstructure. Ph.D. thesis, LMS, École Polytechnique: http://www.polymedia.polytechnique.fr/Center.cfm?Table=These.

Danas, K., Idiart, M.I., Ponte Castañeda, P., 2008a. A homogenization-based constitutive model for two-dimensional viscoplastic porous media. C. R. Mecanique 336, 79–90.

Danas, K., Idiart, M.I., Ponte Castañeda, P., 2008b. A homogenization-based constitutive model for isotropic viscoplastic porous media. Int. J. Solids Struct. 45, 3392–3409.

Duva, J.M., 1986. A constitutive description of nonlinear materials containing voids. Mech. Mater. 5, 137–144.

Duva, J.M., Hutchinson, J.W., 1984. Constitutive potentials for dilutely voided nonlinear materials. Mech. Mater. 3, 41–54.

Eshelby, J.D., 1957. The determination of the elastic field of an ellipsoidal inclusion and related problems. Proc. R. Soc. Lond. A 241, 376–396.

Flandi, L., Leblond, J.-B., 2005a. A new model for porous nonlinear viscous solids incorporating void shape effects – I: Theory. Eur. J. Mech. A/Solids 24, 537–551.

Flandi, L., Leblond, J.-B., 2005b. A new model for porous nonlinear viscous solids incorporating void shape effects – II: Numerical validation. Eur. J. Mech. A/Solids 24, 552–571.

Fleck, N.A., Hutchinson, J.W., 1986. Void growth in shear. Proc. R. Soc. Lond. A 407, 435–458.

Gărăjeu, M., Michel, J.-C., Suquet, P., 2000. A micromechanical approach of damage in viscoplastic materials by evolution in size, shape and distribution of voids. Comput. Methods Appl. Mech. Engrg. 183, 223–246.

Gologanu, M., Leblond, J.-B., Devaux, J., 1993. Approximate models for ductile metals containing non-spherical voids – case of axisymmetric prolate ellipsoidal cavities. J. Mech. Phys. Solids 41, 1723–1754.

Gologanu, M., Leblond, J.-B., Devaux, J., 1994. Approximate models for ductile metals containing non-spherical voids – case of axisymmetric oblate ellipsoidal cavities. ASME J. Engrg. Mater. Technol. 116, 290–297.

Gologanu, M., Leblond, J.-B., Devaux, J., 1997. Recent extensions of Gurson's model for porous ductile metals. In: Suquet, P. (Ed.), Continuum Micromechanics. In: CISM Lectures Series. Springer, New York, pp. 61–130.

Gologanu, M., Leblond, J.-B., Perrin, G., Devaux, J., 2001a. Theoretical models for voids coalescence in porous ductile solids. I. Coalescence "in layers". Int. J. Solids Struct. 38, 5581–5594.

Gologanu, M., Leblond, J.-B., Perrin, G., Devaux, J., 2001b. Theoretical models for voids coalescence in porous ductile solids. II. Coalescence "in columns". Int. J. Solids Struct. 38, 5595–5604.

Gurson, A.L., 1977. Continuum theory of ductile rupture by void nucleation and growth. J. Engrg. Mater. Technol. 99, 2–15.

Hashin, Z., 1962. The elastic moduli of heterogeneous materials. J. Appl. Mech., 143–150.

Hashin, Z., Shtrikman, S., 1963. A variational approach to the theory of the elastic behavior of multiphase materials. J. Mech. Phys. Solids 11, 127–140.

Hill, R., 1956. New horizons in the mechanics of solids. J. Mech. Phys. Solids 5, 66–74.

Hill, R., 1963. Elastic properties of reinforced solids: some theoretical principles. J. Mech. Phys. Solids 11, 127–140.

Hill, R., 1978. Aspects of invariance in solids mechanics. In: Yih, C.-S. (Ed.), Advances in Applied Mechanics, vol. 18. Academic Press, New York, pp. 1–75.

Huang, R., 1991. Accurate dilatation rates for spherical voids in triaxial stress fields. J. Appl. Mech. 58, 1084–1086.

Huang, R., Hutchinson, J., Tveergard, W.V., 1991. Cavitation instabilities in elastic-plastic solids. J. Mech. Phys. Solids 39, 223–241.

Idiart, M.I., Danas, K., Ponte Castañeda, P., 2006. Second-order estimates for nonlinear composites and application to isotropic constituents. C. R. Mecanique 334, 575–581.

Idiart, M.I., Ponte Castañeda, P., 2005. Second-order estimates for nonlinear isotropic composites with spherical pores and rigid particles. C. R. Mecanique 333, 147–154.

Idiart, M.I., Ponte Castañeda, P., 2007. Field statistics in nonlinear composites. I: Theory. Proc. R. Soc. Lond. A 463, 183–202.

Kailasam, M., Aravas, N., Ponte Castañeda, P., 2000. Porous metals with developing anisotropy: Constitutive models, computational issues and applications to deformation processing. Comput. Modelling Engrg. Sci. 1, 105–118.

Kailasam, M., Ponte Castañeda, P., 1998. A general constitutive theory for linear and nonlinear particulate media with microstructure evolution. J. Mech. Phys. Solids 46, 427–465.

Klöcker, H., Tveergard, V., 2003. Growth and coalescence of non-spherical voids in metals deformed at elevated temperature. Int. J. Mech. Sci. 45, 1283–1308.

Leblond, J.-B., Mottet, G., 2008. A theoretical approach of strain localization within thin planar bands in porous ductile materials. C. R. Mecanique 336, 176–189.

Leblond, J.-B., Perrin, G., Suquet, P., 1994. Exact results and approximate models for porous viscoplastic solids. Int. J. Plasticity 10, 213–235.

Lee, B.J., Mear, M.E., 1992a. Effective properties of power-law solids containing elliptical inhomogeneities. Part II: Voids. Mech. Mater. 13, 337–356.

Lee, B.J., Mear, M.E., 1992b. Axisymmetric deformation of power-law solids containing a dilute concentration of aligned spheroidal voids. J. Mech. Phys. Solids 40, 1805–1836.

Lee, B.J., Mear, M.E., 1994. Studies of the growth and collapse of voids in viscous solids. J. Engrg. Mater. Technol. 116, 348–358.

Lee, B.J., Mear, M.E., 1999. Evolution of elliptical voids in power-law viscous solids. Mech. Mater. 31, 9–28.

Levin, V.M., 1967. Thermal expansion coefficients of heterogeneous materials. Mekh. Tverd. Tela 2, 83–94.

McClintock, F.A., 1968. A criterion by for ductile fracture by growth of holes. Trans. ASME, Ser. E, J. Appl. Mech. 35, 363–371.

Michel, J.-C., Suquet, P., 1992. The constitutive law of nonlinear viscous and porous materials. J. Mech. Phys. Solids 40, 783–812.

Monchiet, V., Charkaluk, E., Kondo, D., 2007. An improvement of Gurson-type models of porous materials by using Eshelby-like trial velocity fields. C. R. Mecanique 335, 32–41.

Nahshon, K., Hutchinson, J.W., 2008. Modification of the Gurson model for shear failure. Eur. J. Mech. A/Solids 27, 1–17.

Pastor, J., Ponte Castañeda, P., 2002. Yield criteria for porous media in plane strain: second-order estimates versus numerical results. C. R. Mecanique 330, 741–747.

Pardoen, T., Hutchinson, J.W., 2000. An extended model for void growth and coalescence. J. Mech. Phys. Solids 48, 2467–2512.

Ponte Castañeda, P., 1991. The effective mechanical properties of nonlinear isotropic composites. J. Mech. Phys. Solids 39, 45–71.

Ponte Castañeda, P., 1992. New variational principles in plasticity and their application to composite materials. J. Mech. Phys. Solids 40, 1757–1788.

Ponte Castañeda, P., 1996. Exact second-order estimates for the effective mechanical properties of nonlinear composite materials. J. Mech. Phys. Solids 44, 827–862.

Ponte Castañeda, P., 2002a. Second-order homogenization estimates for nonlinear composites incorporating field fluctuations. I. Theory. J. Mech. Phys. Solids 50, 737–757.

Ponte Castañeda, P., 2002b. Second-order homogenization estimates for nonlinear composites incorporating field fluctuations. II. Applications. J. Mech. Phys. Solids 50, 759–782.

Ponte Castañeda, P., 2006. Heterogenous Materials. Ecole Polytechnique editions.

Ponte Castañeda, P., Suquet, P., 1998. Nonlinear composites. Adv. Appl. Mech. 34, 171–302.

Ponte Castañeda, P., Willis, J.R., 1995. The effect of spatial distribution on the effective behavior of composite materials and cracked media. J. Mech. Phys. Solids 43, 1919–1951.

Ponte Castañeda, P., Zaidman, M., 1994. Constitutive models for porous materials with evolving microstructure. J. Mech. Phys. Solids 42, 1459–1497.

Rice, J.R., Tracey, D.M., 1969. On the ductile enlargement of voids in triaxial fields. J. Mech. Phys. Solids 17, 201–217.

Suquet, P., 1983. Analyse limite et homgénéisation. C. R. Acad. Sci. Paris II 296, 1355–1358.

Suquet, P., 1993. Overall potentials and extremal surfaces of power law or ideally plastic materials. J. Mech. Phys. Solids 41, 981–1002.

Suquet, P., 1995. Overall properties of nonlinear composites: a modified secant moduli theory and its link with Ponte Castañeda's nonlinear variational procedure. C. R. Acad. Sci. Paris II 320, 563–571.

Talbot, D.R.S., Willis, J.R., 1985. Variational principles for inhomogeneous nonlinear media. IMA J. Appl. Math. 35, 39–54.

Talbot, D.R.S., Willis, J.R., 1992. Some simple explicit bounds for the overall behavior of nonlinear composites. Int. J. Solids Struct. 29, 1981–1987.

Tvergaard, V., 1981. Influence of voids on shear band instabilities under plane strain conditions. Int. J. Fracture 17, 389–407.

Willis, J.R., 1977. Bounds and self-consistent estimates for the overall moduli of anisotropic composites. J. Mech. Phys. Solids 25, 185–202.
Willis, J.R., 1978. Variational principles and bounds for the overall properties of composites. In: Provan, J. (Ed.), Continuum Models and Discrete Systems, vol. 2. University of Waterloo Press, pp. 185–212.
Willis, J.R., 1991. On methods for bounding the overall properties of nonlinear composites. J. Mech. Phys. Solids 39, 73–86.
Xue, L., 2008. Constitutive modeling of void shearing effect in ductile fracture of porous materials. Eng. Frac. Mech. 75, 3343–3366.